

CLoG: Benchmarking Continual Learning of Image Generation Models

Haotian Zhang^{*1}, Junting Zhou^{*1}, Haowei Lin^{*1}, Hang Ye^{*1}, Jianhua Zhu^{*1},
Zihao Wang¹, Liangcai Gao¹, Yizhou Wang¹ and Yitao Liang¹

¹Peking University

Continual Learning (CL) poses a significant challenge in Artificial Intelligence, aiming to mirror the human ability to incrementally acquire knowledge and skills. While extensive research has focused on CL within the context of classification tasks, the advent of increasingly powerful generative models necessitates the exploration of Continual Learning of Generative models (CLoG). This paper advocates for shifting the research focus from classification-based CL to CLoG. We systematically identify the unique challenges presented by CLoG compared to traditional classification-based CL. We adapt three types of existing CL methodologies—replay-based, regularization-based, and parameter-isolation-based methods—to generative tasks and introduce comprehensive benchmarks for CLoG that feature great diversity and broad task coverage. Our benchmarks and results yield intriguing insights that can be valuable for developing future CLoG methods. Additionally, we will release a codebase designed to facilitate easy benchmarking and experimentation in CLoG publicly at <https://github.com/linhaowei1/CLoG>. We believe that shifting the research focus to CLoG will benefit the continual learning community and illuminate the path for next-generation AI-generated content (AIGC) in a lifelong learning paradigm.

1. Introduction

The development of Artificial Intelligence Generated Content (AIGC) marks a paradigm shift from classification-based applications, such as image recognition (He et al., 2016; Kolesnikov et al., 2021; Krizhevsky et al., 2012; Simonyan and Zisserman, 2014; Szegedy et al., 2015) and text classification (Jiang et al., 2016; Kalchbrenner et al., 2014; Kowsari et al., 2017; Lai et al., 2015; Minaee et al., 2021; Yang et al., 2016), to powerful generative models. Advances in generative learning, including GANs (Goodfellow et al., 2014; Karras et al., 2019; Park et al., 2019; Radford et al., 2016; Zhu et al., 2020) and diffusion models (Ho et al., 2020b; Sohl-Dickstein et al., 2015; Song et al., 2021), have enabled AI to create novel content, such as images (Dhariwal and Nichol, 2021b; Ho et al., 2020b; Isola et al., 2018; Ramesh et al., 2021; Rombach et al., 2022; Saharia et al., 2022), music (Donahue et al., 2019; Huang et al., 2018; van den Oord et al., 2016; Yu et al., 2021), video (Anonymous, 2022; Lu et al., 2023; Singer et al., 2023; Wang et al., 2024; Xing et al., 2023), and molecules (Jing et al., 2022; Xu et al., 2022). This shift significantly broadens AI’s impact across various fields in both industry and daily life.

Continual learning (CL), which involves AI systems incrementally mastering a sequence of tasks $\mathcal{T}^{(1)}, \mathcal{T}^{(2)}, \dots, \mathcal{T}^{(T)}$ (Delange et al., 2021; Ke and Liu, 2023), is a crucial and well-regarded challenge in AI research. A main assumption of continual learning is that once a task is learned, its training data becomes inaccessible, leading to a phenomenon known as *catastrophic forgetting* (CF) (McCloskey and Cohen, 1989a). Catastrophic forgetting is characterized by a decline in performance on previously learned tasks due to updates in model parameters during the acquisition of new tasks (Delange et al., 2021; Ke and Liu, 2023; McCloskey and Cohen, 1989a). Recent advancements have significantly mitigated CF in various continual learning settings (Ke et al., 2021, 2022; Madotto et al., 2021; Serrà et al., 2018; Sun et al., 2020; Wortsman et al., 2020a), however, most existing CL approaches and frameworks have been tailored primarily for *classification-based models* (Van de Ven and Tolias,

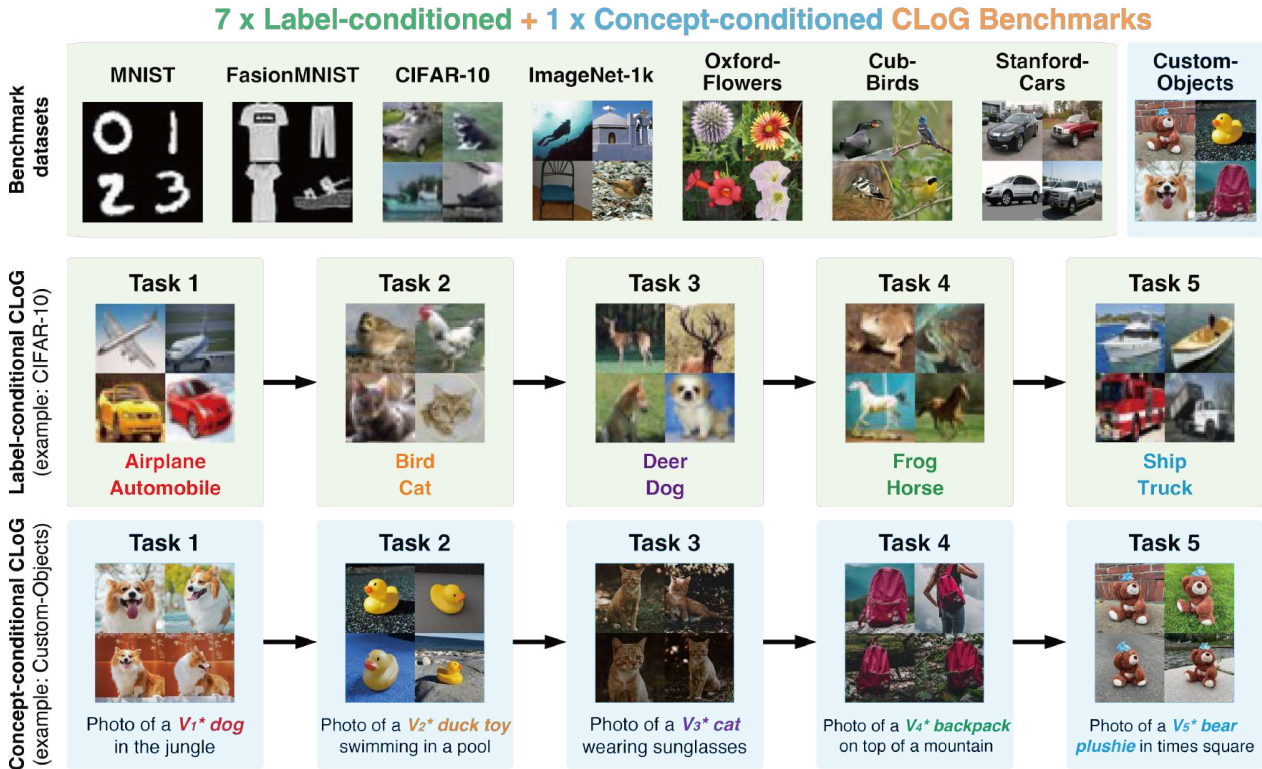


Figure 1 | **Overview of benchmarks.** Seven label-conditioned and one concept-conditioned CLoG benchmarks are studied, with details presented in Table 1 and Section 3.1. *Label-conditioned CLoG* learns a sequence of generation tasks conditioned on label indices. *Concept-conditioned CLoG* learns to synthesize a sequence of concepts (denoted as V_i^* for the i th concept) given arbitrary text prompts.

2019). Given the rising importance of generative models, we believe that *now is an opportune time to pivot the research focus of CL community towards the Continual Learning of Generative models (CLOG)*. Compared to classification-based CL that often learns a sequence of categorical distributions (*i.e.*, classification tasks) via standard classifier architecture (encoder + classification head) (Lin et al., 2024b; Wang et al., 2022; Yan et al., 2021), CLoG typically necessitates the use of sophisticated generative models, such as VAE (Kingma and Welling, 2013), GAN (Goodfellow et al., 2014), or score-based models (Song et al., 2020b), to model the complicated data distributions. The diverse model architectures, which are generally more complex to optimize or incrementally expand during continual learning, make CLoG a more challenging setting than classification-based CL.

The earliest related work of CLoG proposes *generative replay* (GR) (Shin et al., 2017) for classification-based CL. GR utilizes a continually trained generator to synthesize data from previous tasks, thereby preventing forgetting when training a continual learning classifier. The primary goal of GR methods, however, is to enhance classification performance rather than the quality of the generated data. In past years, pioneering studies in CLoG have emerged (Cong et al., 2020a; Sun et al., 2024; Zhai et al., 2019), but they often lacked a unified evaluation protocol and tested on distinctive distinct tasks, making the comparison difficult. Additionally, the diversity in model architectures, data processing techniques, training pipelines, and evaluation metrics complicates fair comparisons between different CLoG methods. This contrasts with classification-based CL, where these choices are relatively

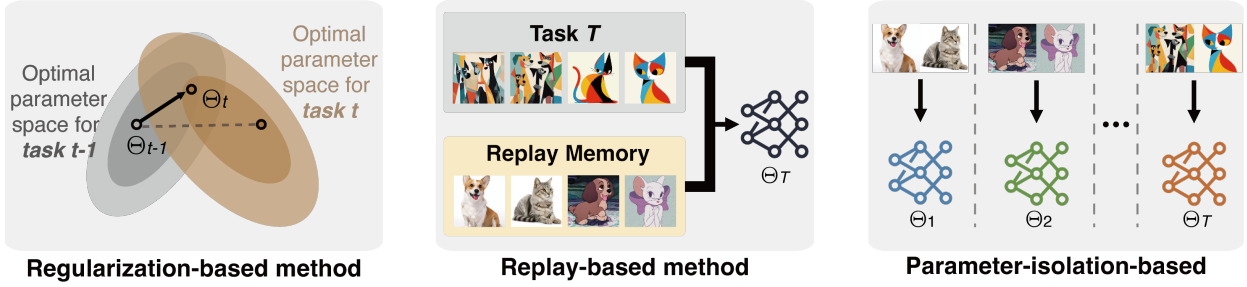


Figure 2 | **Overview of baselines.** Three types of CL baselines are adapted to CLoG, which include *regularization-based*, *replay-based*, and *parameter-isolation-based* methods, resulting in a total of twelve different CLoG baselines. The detailed information on the baselines are in Section 3.2.

standardized (De Lange et al., 2021; Lomonaco et al., 2021; Wang et al., 2023).

In this paper, we establish a foundational framework for studying CLoG. Initially, we define the problem of CLoG and delve deeply into it by leveraging insights from the existing research on classification-based CL (Section 2). We then meticulously develop benchmarks for CLoG, focusing on task selection (Section 3.1), baseline setup (Section 3.2), metrics design (Section 3.3), and training specifics (Section 3.4). Our benchmarks are designed to encompass a broad spectrum of tasks and scenarios, which include varying image resolutions, knowledge transfer capabilities, sizes of training sets, and input conditions, etc. We maintain a clean baseline set by adapting representative CL methods to CLoG, employ unified evaluation metrics, and enhance the efficiency of evaluation process by focusing only on the specifics crucial for CL. Our benchmarks provide valuable insights and are intended to inspire further advancements in CLoG methodologies. We will also release our extensible codebase for the benefit of CLoG research to the public.

In addition to establishing a foundational framework for CLoG, this paper also aims to reflect on current CL research. The shift from classification-based CL to CLoG is driven by the emergence of generative foundation models (e.g., Sora (Brooks et al., 2024), GPT-4 (Achiam et al., 2023), Gemini (Team et al., 2023)), which integrate task-specific models into a unified generalist framework. As traditional CL methods primarily focus on discrete tasks, the development of CL methods that are tailored for foundation models presents an urgent and relevant challenge. Additionally, we discuss the potential applications of CLoG in diverse modalities and outline several promising directions for future advancements in CLoG methodologies.

2. From Traditional CL to CLoG

In this section, we offer an overview of continual learning (CL). We will discuss the “three-types” of CL methods: regularization-based, replay-based, and parameter-isolation-based methods in Section 2.1. Then we will contextualize the approach and insights into continual learning for generative models (CLoG) within the existing framework of CL research, as detailed in Section 2.2.

2.1. Continual Learning

Formulation of general CL. CL learns a sequence of tasks $\mathcal{T}^{(1)}, \mathcal{T}^{(2)}, \dots, \mathcal{T}^{(T)}$ incrementally. Each task $\mathcal{T}^{(t)}$ has an input space $\mathcal{X}^{(t)}$, an output space $\mathcal{Y}^{(t)}$, and a training set $\mathcal{D}^{(t)} = \{(\mathbf{x}_j^{(t)}, \mathbf{y}_j^{(t)})\}_{j=1}^{|\mathcal{D}^{(t)}|}$ drawn *i.i.d.* from distribution $\mathcal{P}_{\mathcal{X}^{(t)} \mathcal{Y}^{(t)}}$. The goal of continual learning is to learn a function $f : \cup_{t=1}^T \mathcal{X}^{(t)} \rightarrow \cup_{t=1}^T \mathcal{Y}^{(t)}$ that can achieve good performance on each task $\mathcal{T}^{(t)}$.

A main assumption of CL is that once a task is learned, its training data $\mathcal{D}^{(t)}$ is no longer accessible

(or with limited access). This assumption simulates the learning process of humans but also causes *catastrophic forgetting* for machine learning models, which refers to performance degradation of previous tasks due to parameter updates in learning each new task (McCloskey and Cohen, 1989b). The existing CL methods which aim to prevent forgetting can be roughly categorized into three types:

(1) **Regularization-based Methods:** The idea of this family is to add regularization to penalize changes to important parameters learned for previous tasks in learning a new task (Aljundi et al., 2018; Chaudhry et al., 2018a; Kirkpatrick et al., 2017; Li and Hoiem, 2017; Zenke et al., 2017).

(2) **Replay-based Methods:** These methods store a small subset of training data from previous tasks (Chaudhry et al., 2019; Kemker and Kanan, 2017; Lopez-Paz and Ranzato, 2017; Rebuffi et al., 2017; Riemer et al., 2018) or learn a data generator to synthesize pseudo data (Cong et al., 2020b; Shin et al., 2017; Wu et al., 2018a; Zhu et al., 2021) of previous tasks. The saved data, the synthesized data, and the new task data are both used in training.

(3) **Parameter-isolation Based Methods:** These methods allocate task-specific parameters to prevent subsequent tasks from interfering the previously learned parameters (Aljundi et al., 2017; Fernando et al., 2017; Lin et al., 2024b; Masana et al., 2021; Rusu et al., 2016; Serra et al., 2018; Wortsman et al., 2020b).

2.2. Continual learning of generative models (CLOG)

Formulation of CLOG. CLOG learns a sequence of generation tasks $\mathcal{T}^{(1)}, \mathcal{T}^{(2)}, \dots, \mathcal{T}^{(T)}$ incrementally. Each task $\mathcal{T}^{(t)}$ has an input space $\mathcal{X}^{(t)}$ (generation conditions) and output space \mathcal{Y} (generation targets), and a training set $\mathcal{D}^{(t)} = \{(\mathbf{x}_j^{(t)}, \mathbf{y}_j^{(t)})\}_{j=1}^{|\mathcal{D}^{(t)}|}$ drawn *i.i.d.* from distribution $\mathcal{P}_{\mathcal{X}^{(t)} \times \mathcal{Y}^{(t)}}$. The goal of CLOG is to learn a mapping $f: \cup_{t=1}^T \mathcal{X}^{(t)} \rightarrow \cup_{t=1}^T \mathcal{Y}^{(t)}$ that can achieve good performance on each task $\mathcal{T}^{(t)}$. The generation conditions can be in various forms such as text (Li et al., 2019; Zhang et al., 2023b), images (Zhai et al., 2021; Zhang et al., 2023b), or label indices (Ho and Salimans, 2021), while the generation targets can be various modalities such as images (Ramesh et al., 2021; Saharia et al., 2022), audio (Huang et al., 2018; van den Oord et al., 2016), or 3D objects (Shi et al., 2023; Zeng et al., 2022). As an initial step towards CLOG, we only focus on image generation conditioned on text or label indices in this paper.

Comparison between CLOG and classification-based CL. The key difference between classification and generative tasks lies in the input space \mathcal{X} and output space \mathcal{Y} . In image generation, the input \mathbf{x} may be some label conditions (*e.g.*, one-hot class) or instructions (text or images), and the output $\mathbf{y} \in \mathbb{R}^{C \times H \times W}$ should be images (C, H, W denote the number of channels, height, and width). CLOG is more challenging as its output space inherently possesses a significantly larger cardinality, while the output of classification-based CL is typically limited to discrete class indices. Thus the model architectures also diverge; classification-based CL typically requires only a simple mechanism to model a categorical distribution, such as a linear mapping or MLP head (Popescu et al., 2009), while CLOG necessitates the use of more sophisticated generative models, such as VAE (Kingma and Welling, 2013), GAN (Goodfellow et al., 2014), or score-based models (Song et al., 2020b). These generative models are generally more complex to optimize and incrementally expand within a continual learning framework compared to classification architectures (Roth et al., 2017; Song and Ermon, 2020).

Remarks on text generation in CL. CL of text generation tasks (Shi et al., 2024; Wu et al., 2024) has garnered increasing interest in the so-called “post-LLM era” (Lin et al., 2024a). Including CL of text generation tasks in CLOG is logical, given their generative nature. However, text generation

typically operates under the framework of “next token prediction” (Radford et al., 2019), which substantially differs from the typical probabilistic generative models. Specifically, text generation models the conditional data distribution, $\mathbf{P}(y|\mathbf{x})$, through autoregressive generation of the form $\prod_{j=1}^{|\mathbf{y}|} \mathbf{P}(y_j|y_1, y_2, \dots, y_{j-1}, \mathbf{x})$, with y_0 representing the “start of sentence” token and y_j the j th token of \mathbf{y} . This approach simplifies the modeling of complex data distributions into predicting a sequence of categorical distributions over the vocabulary space. Existing studies have shown that text generation tasks tend to exhibit less forgetting when integrated into CL frameworks, indicating a potentially smoother adaptation to continual learning (Cao et al., 2024; Shao et al., 2023; Yin et al., 2022). While we advocate for the inclusion of text generation in CLOG due to its alignment with CLOG’s formulation, the primary focus of this paper remains on general probabilistic generative modeling due to its broader applications and the insufficient attention it has received in research.

3. Benchmark Design

In this section, we show how to design a foundational benchmark for the study of CLOG. Our design framework is structured around four key research questions, which are addressed in each subsection:

- (Q₁) *How can we select CLOG tasks that are both diverse and representative?*
- (Q₂) *How should we establish baselines, considering the current advancements in CL research?*
- (Q₃) *What metrics should be employed to effectively and efficiently assess the CLOG methods?*
- (Q₄) *How can we implement different CLOG methods fairly, given the variety of training specifics?*

3.1. Task selection

The fundamental criterion for choosing tasks for our benchmark is to ensure they are *diverse* and *representative*. Diversity is crucial for evaluating the CLOG methods across various dimensions, making them relevant for different real-world applications. Selecting representative tasks is essential for efficiency since executing numerous redundant tasks can be resource-intensive and unproductive.

Datasets We follow traditional CL literature (Buzzega et al., 2020; Kim et al., 2022; Lin et al., 2024b; Rebuffi et al., 2017; Wang et al., 2022) to split a publicly available dataset into a sequence of tasks for CLOG. The *training datasets* are summarized in Table 1 and introduced as follows. **MNIST** (LeCun et al., 2010) contains 60,000 grayscale images of handwritten digits (0-9) in a 28×28 pixel format. We resize the images to 32×32 resolution for image generation. **FasionMNIST** (Xiao et al., 2017a) consists of 60,000 grayscale images across 10 fashion categories, such as shirts, dresses, and shoes. The images are also resized from 28×28 to 32×32 for image generation. **CIFAR-10** (Krizhevsky et al., 2009) consists of 60,000 colored images sized at 32×32 pixels, divided into 10 classes including airplane, automobile, bird, cat, deer, dog, frog, horse, ship, and truck. **ImageNet-1k** (Russakovsky et al., 2015) is the most commonly used subset of ImageNet, which spans 1000 classes and contains 1,281,167 training images. We use the down-sampled 64×64 version following Chrabaszcz et al. (2017). **Oxford-Flower** (Nilsback and Zisserman, 2008) consists of 102 flower categories that commonly occur in the United Kingdom. Each class consists of between 40 and 258 images, with a total of 7,169 images. The images are resized to 128×128 for generation. **CUB-Birds** (Wah et al., 2011) contains 11,788 images of 200 subcategories belonging to birds, which is a widely-used dataset for fine-grained visual categorization task. We resize the images to 128×128 for generation. **Stanford-Cars** (Krause et al., 2013) consists of 196 classes of cars with a total of 8,144 images. The images are also resized to 128×128 for image generation. **Custom-Objects** (Sun et al., 2024) contains 5 customized concepts from users with paired text-image demonstrations. Each concept has

Table 1 | The detailed configurations of eight CLOG benchmarks studied in this paper.

Dataset	Image Resolution	#Training Images per Task	#Tasks	Description of Each Task
MNIST (LeCun et al., 2010)	32×32	12,000	5	Conditional generation of 2 classes of handwritten digits
FashionMNIST (Xiao et al., 2017a)	32×32	12,000	5	Conditional generation of 2 classes of fashion products
CIFAR-10 (Krizhevsky et al., 2009)	32×32	10,000	5	Conditional generation of 2 classes of common objects
ImageNet-1k (Russakovsky et al., 2015)	64×64	~64,000	20	Conditional generation of 50 classes of ImageNet images
Oxford-Flower (Nilsback and Zisserman, 2008)	128×128	~1,400	5	Conditional generation of 20 categories of flowers
CUB-Birds (Wah et al., 2011)	128×128	~1,200	10	Conditional generation of 20 species of birds
Stanford-Cars (Krause et al., 2013)	128×128	~600	14	Conditional generation of 14 classes of cars
Custom-Objects (Sun et al., 2024)	512×512	5	5	Generate a customized object given text conditions

5 demonstrations with 512×512 image resolution. The task is to generate the customized concepts given arbitrary text conditions.

Task sequence We partitioned MNIST, FashionMNIST, and CIFAR-10 into five tasks, assigning two classes to each task. ImageNet-1k was divided into 20 tasks with 50 classes per task, Oxford-Flower into five tasks with 20 categories per task, CUB-Birds into 10 tasks with 20 categories per task, Stanford-Cars into 14 tasks with 14 classes per task, and Custom-Objects into five tasks with one object per task. Following the random class order protocol in Rebuffi et al. (2017), we generate five different class orders for each experiment and report their averaged metrics over five random orders. For a fair comparison, the class orderings are fixed in our experiments (see Appendix C.2). It is important to note that one dataset can be segmented into varying numbers of tasks (Lin et al., 2024b) or without requiring uniformity in class (Hemati et al., 2024). These customized CL settings can be explored in the future, and our current benchmark focuses on addressing more fundamental challenges in CLOG for now.

3.2. Baseline setup

To establish the baselines, we adapt the three types of CL techniques (*i.e.*, regularization-based, replay-based, parameter-isolation-based) to CLOG. It is noted that there are several classification-based CL or CLOG methods that combine multiple techniques, but we did not include these baselines in our set as many of their basic components can be unified into the three types of methods (see Appendix A). To facilitate a deeper understanding of each type of the method, we selected twelve representative baselines and two types of generative models (*i.e.*, GAN, Diffusion Models) to initiate our analysis.

Adapted Baselines (1) **Naive Continual Learning (NCL)** means continually training the same model without any CL techniques to deal with forgetting, which is the simplest baseline in CL. (2) **Non-Continual Learning (Non-CL)** means pooling the data from all tasks together and training only one model for all tasks. This is not under a CL setting but its performance can be viewed as an upper bound for CL baselines. (3) **Ensemble** trains a separate model for each task. This baseline is forgetting-free, but the memory consumption is huge when more tasks arrive, and there is no knowledge transfer between different tasks. (4) **Experience Replay (ER)** (Lopez-Paz and Ranzato, 2017) directly combines replay samples and current task samples in training batches to train the model. The replay data is saved by reservoir sampling (Chaudhry et al., 2019; Riemer et al., 2018). (5) **Generative Replay (GR)** (Shin et al., 2017) replaces the replay samples used in ER with generative replay samples. When training a new task in CLOG, the model is copied and the replay samples are generated via the copied model. (6) **Knowledge Distillation (KD)** (Hinton et al., 2015) is a regularization-based method in CL. The model is copied as a fixed teacher model before learning the new task. An ℓ_2 auxiliary loss between the new and old model outputs is added to the NCL objective. (7) **L2** (Smith et al., 2023) is also a regularization-based method and copies the model

before learning a new task. An ℓ_2 distance between the current and copied network parameters is added as an auxiliary loss. (8) **Elastic Weight Consolidation (EWC)** (Kirkpatrick et al., 2017) is also a regularization technique that reweights the ℓ_2 loss for different parameters. The weights are based on the degree of overlap between the two tasks’ Fisher matrices. (9) **Synapse Intelligence (SI)** (Zenke et al., 2017) is a regularization method that is similar to EWC, while the parameter weights are computed by measuring the parameter updating trajectory during training. (10) **Memory Aware Synapses (MAS)** (Aljundi et al., 2018) is also a regularization-based method. It measures the importance of parameters by the magnitude of the gradient and penalizes changes to parameters that are essential to previous tasks. (11) **Averaged Gradient Episodic Memory (A-GEM)** (Chaudhry et al., 2018b) is a regularization-based method that exploits replay data. It prevents the loss increasing on replay samples by gradient projection. (12) **C-LoRA** (Smith et al., 2024) is a parameter-isolation-based CL method that was first designed for concept-conditional CLOG. It overcomes forgetting by learning task-specific LoRA (Hu et al., 2022) upon a pre-trained backbone. We adapt it to from-scratch-training by fully training the backbone on the first task and adopting LoRA tuning in the subsequent tasks.

Generative models We apply CLOG methods on two representative generative models: Generative Adversarial Networks (GAN) (Goodfellow et al., 2014) and Diffusion Models (Ho et al., 2020a). We introduce them in Appendix A.1.

3.3. Metrics design

We found that the existing CLOG literature used many distinct metrics (refer to Appendix A for details), which makes the comparison between different works hard. In this paper, we provide unified metric choices for evaluating CLOG. Suppose $m(f, \mathcal{T})$ is a metric to evaluate the generation quality of a generative model f on a task \mathcal{T} , then we extend the metrics from classification-based CL to evaluate the performance of CLOG. When learning the task sequence $\mathcal{T}^{(1)}, \mathcal{T}^{(2)}, \dots, \mathcal{T}^{(T)}$, we denote the model after learning $\mathcal{T}^{(i)}$ as $f^{(i)}$, then we define the CLOG metrics as follows:

Average Incremental Quality (AIQ) (Douillard et al., 2020; Hou et al., 2019) We first define the average quality (AQ) when the model just learns the t -th task $\mathcal{T}^{(t)}$ as $AQ^{(t)} = \frac{1}{t} \sum_{i=1}^t m(f^{(t)}, \mathcal{T}^{(i)})$. Then the *average incremental quality* (AIQ) is defined to evaluate the historical performance as $AIQ = \frac{1}{T} \sum_{t=1}^T AQ^{(t)}$.

Average Final Quality (AFQ) (Chaudhry et al., 2018a; Lopez-Paz and Ranzato, 2017) Since AIQ evaluates the historical performance of the model during CL, while in downstream applications we may only care about the final performance of the model (i.e., the performance of $f^{(T)}$), *average final quality* (AFQ) is defined as $AFQ = AQ^{(T)}$.

Forgetting Rate (FR) (Chaudhry et al., 2018a; Lopez-Paz and Ranzato, 2017) Apart from AIQ and AFQ that measure the learned “knowledge” or “ability” of the model, measuring the capability to preserve the learned “knowledge” or “ability” during the continual learning process is also important. The *forgetting rate* (FR) of task $\mathcal{T}^{(t)}$ can be calculated by the difference between the current performance $m(f^{(T)}, \mathcal{T}^{(t)})$ and the performance when the model first learns this task $m(f^{(t)}, \mathcal{T}^{(t)})$:

$$FR = \begin{cases} \frac{1}{T-1} \sum_{t=1}^{T-1} (m(f^{(T)}, \mathcal{T}^{(t)}) - m(f^{(t)}, \mathcal{T}^{(t)})) & \text{(if larger } m \text{ is better)} \\ \frac{1}{T-1} \sum_{t=1}^{T-1} (m(f^{(t)}, \mathcal{T}^{(t)}) - m(f^{(T)}, \mathcal{T}^{(t)})) & \text{(if smaller } m \text{ is better)} \end{cases} \quad (1)$$

For label-conditioned CLoG, we choose Fréchet inception distance (FID) (Heusel et al., 2017) as quality metric $m(f, \mathcal{T})$ (smaller m is better), which is commonly used to assess the generation quality of image generation models (Ho et al., 2020a; Song et al., 2020a).¹ For concept-conditioned CLoG, we follow DreamBooth (Ruiz et al., 2023) to compute the CLIP alignment score (Radford et al., 2021) between generated image and the provided concept (image alignment score), and between generated image and the text prompts (text alignment score), respectively. The two scores are averaged to obtain a single quality metric for easy comparison.

3.4. Training specifics

To ensure a fair comparison across different CLoG methods, given the diverse training specifics (e.g., image augmentation techniques, network configurations, and other training tricks), a unified protocol is necessary. *The key idea of this paper is to fix the specifics that are irrelevant to CL performance (which might otherwise affect the generation performance) in implementing CLoG baselines.* Specifically, we fix the backbone for GAN and Diffusion Models to StyleGAN2 (Karras et al., 2020b) and DDIM (Song et al., 2020a) for label-conditioned CLoG, DreamBooth (Ruiz et al., 2023) and Custom Diffusion (Kumari et al., 2023) for concept-conditioned CLoG. We fix CL-irrelevant configurations such as DDIM steps, condition encoding, image augmentation, or exponential moving average tricks (Karras et al., 2017), with full details presented in Appendix C. This standardization improves evaluation efficiency by significantly reducing the hyper-parameter space, allowing us to focus on optimizing the hyper-parameters crucial for CL.

4. Experiments

4.1. Implementation Details

To ensure the fair comparison across methods, we follow Section 3.4 to use unified settings with common hyperparameters and architecture choices. We follow Heusel et al. (2017) to compute FID using the entire training dataset as reference images. To achieve the best training performance, we compute the quality metrics on current task every 500 steps and save the best checkpoint. If the method has CL-related hyper-parameters (e.g., regularization weights), we will search for 8 values across different magnitudes and pick the hyper-parameter based on the quality metrics. We found it’s hard to train GAN on the long-sequence and large-scale ImageNet-1k benchmark, so we leave it as “NA” (Not A Number). We didn’t implement C-LoRA on GAN and Custom Diffusion as it is not applicable. We follow Lin et al. (2024b) to use reservoir replay buffer (Vitter, 1985) for ER with buffer sizes as 5000 samples for ImageNet-1k, and 200 for the other label-conditioned CLoG benchmarks. Replay-based methods are excluded in Custom-Object as it has very few training samples and thus replay is equivalent to Non-CL. We will present more specific implementation details in Appendix C.

4.2. Result Analysis

We present the AFQ results as Tables 2 and 3, and postpone the AIQ, FR results in Appendices B.2 and B.4. We also conduct additional study on different configurations such as DDIM steps, replay buffer size, different task numbers within the same dataset, different alignment score metrics in Appendix B.1, and visualize the generation results, compare the method efficiency in Appendices B.3 and B.5. We jointly analyze these results and draw some observations as follows.

¹Some existing CLoG works used pre-trained classifiers to compute the accuracy of conditional generation, while we find it unsuitable for CLoG and do not adopt it. For example, a pre-trained classifier is not always available for some datasets, and the classifiers often assign wrong prediction for OOD generated images.

Table 2 | **AFQ results for label-conditioned CLOG benchmarks.** The best result in each column with the same architecture (StyleGAN2, DDIM) is highlighted in **red**, while the second best and third best are highlighted in **blue** and **yellow**, respectively. The quality metric is FID (*the lower value is better*). We average each AFQ value on 5 class orders and show the standard deviations as superscripts. We use dashlines to split different categories of baselines (Non-CL & NCL, replay-based, regularization-based, parameter-isolation-based).

	MNIST	Fashion-MNIST	CIFAR-10	CUB-Birds	Oxford-Flowers	Stanford-Cars	ImageNet-1k
- StyleGAN2							
Non-CL	41.19 ^{+3.44}	66.53 ^{+1.46}	63.02 ^{+5.18}	48.36 ^{+2.16}	99.50 ^{+10.4}	33.68 ^{+2.95}	NA
NCL	60.98 ^{+6.13}	94.10 ^{+13.20}	103.34 ^{+10.59}	112.57 ^{+23.05}	131.98 ^{+16.39}	68.20 ^{+2.05}	NA
ER	87.91 ^{+24.33}	133.24 ^{+35.98}	236.44 ^{+11.18}	175.99 ^{+20.19}	134.94 ^{+2.55}	147.88 ^{+6.00}	NA
GR	113.37 ^{+38.97}	115.18 ^{+26.15}	128.81 ^{+8.37}	189.27 ^{+11.55}	161.96 ^{+10.80}	161.55 ^{+27.85}	NA
KD	55.04 ^{+4.88}	86.94 ^{+4.05}	105.73 ^{+13.27}	108.68 ^{+11.16}	120.66 ^{+17.47}	80.45 ^{+4.02}	NA
L2	63.15 ^{+13.15}	113.41 ^{+7.12}	108.52 ^{+6.24}	191.43 ^{+17.52}	158.55 ^{+11.97}	201.80 ^{+32.95}	NA
EWC	54.73 ^{+4.52}	87.20 ^{+11.12}	95.33 ^{+19.04}	156.06 ^{+13.38}	131.62 ^{+6.00}	100.22 ^{+10.81}	NA
SI	93.12 ^{+17.59}	102.29 ^{+7.57}	100.13 ^{+4.85}	204.44 ^{+14.61}	170.53 ^{+15.07}	211.72 ^{+46.52}	NA
MAS	57.89 ^{+8.53}	86.86 ^{+5.29}	85.22 ^{+2.83}	186.34 ^{+17.63}	144.31 ^{+14.99}	149.11 ^{+19.21}	NA
A-GEM	41.51 ^{+16.42}	85.37 ^{+18.99}	98.42 ^{+11.47}	116.37 ^{+13.30}	127.93 ^{+12.64}	75.46 ^{+5.54}	NA
Ensemble	8.64 ^{+1.74}	27.76 ^{+0.37}	45.26 ^{+0.61}	180.71 ^{+2.46}	145.59 ^{+1.61}	230.74 ^{+3.93}	NA
- DDIM							
Non-CL	5.59 ^{+3.67}	9.02 ^{+0.23}	30.19 ^{+1.29}	49.30 ^{+4.43}	48.81 ^{+0.84}	27.97 ^{+0.42}	47.27
NCL	115.47 ^{+9.30}	139.81 ^{+19.04}	115.60 ^{+20.51}	98.89 ^{+6.06}	102.98 ^{+16.39}	42.81 ^{+8.91}	91.46
ER	28.64 ^{+2.74}	52.47 ^{+2.85}	132.07 ^{+8.92}	72.53 ^{+6.39}	77.03 ^{+2.62}	81.26 ^{+6.44}	101.15
GR	90.28 ^{+4.72}	34.96 ^{+6.31}	73.15 ^{+2.48}	106.93 ^{+4.67}	180.68 ^{+27.60}	261.59 ^{+3.24}	NA
KD	149.72 ^{+13.17}	233.55 ^{+11.89}	162.13 ^{+16.11}	181.40 ^{+8.86}	176.84 ^{+20.88}	103.06 ^{+12.55}	107.57
L2	184.05 ^{+27.14}	190.04 ^{+5.81}	174.78 ^{+16.90}	182.79 ^{+13.50}	191.90 ^{+33.87}	254.21 ^{+28.00}	119.22
EWC	158.22 ^{+22.70}	139.52 ^{+20.07}	127.09 ^{+19.23}	101.12 ^{+14.87}	99.34 ^{+8.27}	49.02 ^{+2.72}	99.93
SI	182.80 ^{+25.55}	156.63 ^{+22.67}	142.32 ^{+26.74}	113.30 ^{+15.91}	98.04 ^{+7.78}	57.06 ^{+8.39}	100.13
MAS	137.28 ^{+14.51}	162.25 ^{+19.61}	124.31 ^{+10.24}	197.73 ^{+15.76}	213.12 ^{+33.11}	282.49 ^{+14.23}	130.21
A-GEM	86.28 ^{+5.94}	139.46 ^{+5.21}	129.24 ^{+27.59}	105.93 ^{+2.67}	121.27 ^{+10.92}	50.13 ^{+2.44}	100.45
Ensemble	4.12 ^{+0.14}	10.42 ^{+0.02}	36.52 ^{+0.55}	133.32 ^{+2.07}	70.16 ^{+8.67}	202.15 ^{+0.52}	56.97
C-LoRA	9.45 ^{+0.38}	24.83 ^{+5.23}	60.11 ^{+6.15}	148.81 ^{+1.22}	117.11 ^{+7.15}	250.90 ^{+35.87}	79.72

NO single method works well across all settings. We first note that Non-CL is not a CL method since it access all the task data, and is often viewed as the upper bound of CL performance for being forgetting-free and able to transfer knowledge between different tasks. Except for Non-CL, no single method works well on all benchmarks. Specifically, the seemingly best-performing parameter-isolation-based methods (*i.e.*, ensemble, C-LoRA) work well on MNIST, FashionMNIST, CIFAR-10, ImageNet-1k, and Custom-Objects, but fail on Oxford-Flowers, CUB-Birds, and Stanford-Cars. This is because they isolate the parameters for different tasks while knowledge transfer is significant for other baselines on these benchmarks due to the similar features shared across tasks, and each task has too few samples to train a task-specific module. Other than the failure of effective knowledge transfer, parameter-isolation-based methods may also be memory-hungry (see Table 12) as they have to allocate parameters for each new task. While C-LoRA greatly addresses the issue by only allocating few LoRA weights, the issue will be amplified in scenarios where the task sequence is long (e.g., learning millions of new concepts). Above all, the current methods are not satisfactory enough and our CLOG benchmark remains an open challenge for developing new methods.

NCL is comparable to regularization-based methods. Although NCL naively trains on the current task data without any protection to previous learned knowledge, it exhibits similar performance compared to the regularization-based methods on all benchmarks. This indicates that regularization-

Table 3 | **AFQ results for concept-conditioned CLoG benchmark.** The best result in each row with the same base method (DreamBooth, Custom Diffusion) is highlighted in **red**, while the second best and third best are highlighted in **blue** and **yellow**, respectively. The quality metric is the average of text and image alignment scores (*the higher value is better*). The AFQ is also averaged over 5 orders.

Model	NCL	Non-CL	KD	L2	EWC	SI	MAS	Ensemble	C-LoRA
DreamBooth	78.54 \pm 0.53	80.09\pm0.1	78.73 \pm 0.16	79.00 \pm 0.38	79.45\pm0.41	78.54 \pm 0.39	78.00 \pm 0.46	80.09\pm0.25	80.42\pm0.25
Custom Diffusion	79.56 \pm 0.17	80.30\pm0.21	79.71 \pm 0.1	79.92 \pm 0.14	80.10\pm0.05	79.59 \pm 0.27	78.79 \pm 0.18	80.39\pm0.24	-

based methods cannot effectively prevent forgetting. We also found that some of them achieve worse performance than NCL because the regularization makes them hard to learn new tasks, for example, MAS achieves poor AFQ on Oxford-Flowers, Stanford-Cars, and Custom-Objects based on Diffusion Models, but it also has almost zero forgetting (shown in Tables 10 and 11) on these benchmarks. Note that we have grid searched the regularization weights from 0.001 to 10000 according to the prior works (Aljundi et al., 2018; Kirkpatrick et al., 2017; Shao et al., 2023) to ensure a faithful implementation. The failure of regularization-based methods also demonstrates the challenge of CLoG due to the use of sophisticated deep generative models.

Replay-based methods face imbalance issue. Surprisingly, replay-based methods (*i.e.*, ER, GR) don’t always outperform non-exemplar methods on CLoG, which contradicts the common observations in classification-based CL where ER is very effective. We relate this phenomenon to the amplification of *CL imbalance* (Guo et al., 2023) and *data imbalance* (Ahn et al., 2020; Huang et al., 2021): the limited replayed samples have been seen and trained many times which make them easier to learn than new task data, and leads to mode collapse (Srivastava et al., 2017) for previous tasks and low plasticity in learning new tasks. The severe mode collapse can be observed for GAN-based ER (see Appendix B.3 for visualizations). CLoG turns to be more sensitive to these issues than classification-based CL possibly because the modeling of data distribution $p(x)$ is more difficult than classification distribution $p(y|x)$ as discussed in Section 2.2.

Comparison between GAN and Diffusion Models. Generally, GAN is harder to optimize than Diffusion Models on CLoG, with worse Non-CL and Ensemble performance as shown in Table 2. This suggests that Diffusion Models are more promising as the base architecture for CLoG.

Comparison between label-conditioned and concept-conditioned CLoG. It is clear that with pre-trained backbone and fewer training samples, the results on concept-conditioned CLoG exhibit less forgetting, and NCL performance is also strong. The results align with the recent CL works that pre-trained text generation models resist forgetting better (Cao et al., 2024; Shao et al., 2023). However, the visualization results shown in Figures B.8 and B.9 are far from perfect, which means it is still necessary to improve the concept-conditioned CLoG methods in future research.

Method Efficiency. We also report the training time and memory consumption of the CLoG methods in Appendix B.5. It is noted that DDIM-based GR is significantly slow, as generating the replay samples for DDIM requires multiple denoising steps (50 in our implementation). It is also noted that the parameter-isolation-based methods have linearly increasing memory consumption when the number of tasks increases, while other methods only consume constant memory budget.

5. Discussions and Limitations

Discussions There has long been a period that CL research focusing on addressing forgetting for classification tasks, and although many advancements have been achieved in the past years, CL methods are rarely applied in real world applications. With the emergence of various “all-in-one” foundation models, the relevance of focusing mainly on classification-based CL is increasingly questionable. Current trends suggest that generative-based foundation models are poised to become the next generation of AI products, integral to everyday life. In this context, CLOG becomes crucial, addressing how these models of diverse architectures, complex learning objectives, and open-ended domains can continuously learn newly emerged knowledge (Ke et al., 2023; Liu et al., 2023a; Verwimp et al., 2023), cater to personalized needs (Pesovski et al., 2024; Rafieian and Yoganarasimhan, 2023; Shahin et al., 2024), and possibly enhance human-AI alignment in an evolving world (Christian, 2021; Leike et al., 2018; Soares and Fallenstein, 2014). Our benchmark results reveal disappointing performance with traditional CL methods, highlighting a pressing need for refined CLOG strategies for future applications.

Limitations and outlook This study primarily presents initial benchmarks and baselines for CLOG, with a focus on traditional representative methods. Future work will include expanding these benchmarks across a wider range of image generation tasks, incorporating various generative conditions (Zhai et al., 2019; Zhang et al., 2023a), and extending to additional modalities such as molecules (Xu et al., 2022). Although we only include baselines from classification-based CL, it is interesting to design methods specifically for generative models by applying techniques such as classifier-guidance (Dhariwal and Nichol, 2021a), and include more generative models (Liu et al., 2022, 2023b; Peebles and Xie, 2022) other than GAN and Diffusion Models. Our current analysis is based solely on existing datasets; hence, we plan to enhance the scope of concept-conditioned CLOG benchmarks by acquiring and incorporating more diverse datasets and domains. Furthermore, while this paper primarily conducts an empirical investigation, advancing the theoretical framework of CLOG will be crucial for its development and understanding.

6. Conclusion

In this paper, we introduce a foundational framework for studying Continual Learning of Generative Models (CLOG). We explore the challenges that CLOG presents compared to the more popular classification-based CL. We establish unified benchmarks, baselines, evaluation protocols, and specific training guidelines for CLOG. Our findings underscore the necessity for developing more advanced CLOG methods in the future. Additionally, we advocate for a shift in focus from classification-based CL to CLOG, given the growing importance of generative foundation models in current research.

References

- O. J. Achiam, S. Adler, S. Agarwal, L. Ahmad, I. Akkaya, F. L. Aleman, D. Almeida, J. Altschmidt, S. Altman, S. Anadkat, R. Avila, I. Babuschkin, S. Balaji, V. Balcom, P. Baltescu, H. Bao, M. Bavarian, J. Belgum, I. Bello, J. Berdine, G. Bernadett-Shapiro, C. Berner, L. Bogdonoff, O. Boiko, M. Boyd, A.-L. Brakman, G. Brockman, T. Brooks, M. Brundage, K. Button, T. Cai, R. Campbell, A. Cann, B. Carey, C. Carlson, R. Carmichael, B. Chan, C. Chang, F. Chantzis, D. Chen, S. Chen, R. Chen, J. Chen, M. Chen, B. Chess, C. Cho, C. Chu, H. W. Chung, D. Cummings, J. Currier, Y. Dai, C. Decareaux, T. Degry, N. Deutsch, D. Deville, A. Dhar, D. Dohan, S. Dowling, S. Dunning, A. Ecoffet, A. Eleti, T. Eloundou, D. Farhi, L. Fedus, N. Felix, S. P. Fishman, J. Forte, I. Fulford, L. Gao, E. Georges, C. Gibson, V. Goel, T. Gogineni, G. Goh, R. Gontijo-Lopes, J. Gordon, M. Grafstein, S. Gray, R. Greene, J. Gross, S. S. Gu, Y. Guo, C. Hallacy, J. Han, J. Harris, Y. He, M. Heaton, J. Heidecke, C. Hesse, A. Hickey, W. Hickey, P. Hoeschele, B. Houghton, K. Hsu, S. Hu, X. Hu, J. Huizinga, S. Jain, S. Jain, J. Jang, A. Jiang, R. Jiang, H. Jin, D. Jin, S. Jomoto, B. Jonn, H. Jun, T. Kaftan, L. Kaiser, A. Kamali, I. Kanitscheider, N. S. Keskar, T. Khan, L. Kilpatrick, J. W. Kim, C. Kim, Y. Kim, H. Kirchner, J. R. Kiros, M. Knight, D. Kokotajlo, L. Kondraciuk, A. Kondrich, A. Konstantinidis, K. Kosic, G. Krueger, V. Kuo, M. Lampe, I. Lan, T. Lee, J. Leike, J. Leung, D. Levy, C. M. Li, R. Lim, M. Lin, S. Lin, M. Litwin, T. Lopez, R. Lowe, P. Lue, A. A. Makanju, K. Malfacini, S. Manning, T. Markov, Y. Markovski, B. Martin, K. Mayer, A. Mayne, B. McGrew, S. M. McKinney, C. McLeavey, P. McMillan, J. McNeil, D. Medina, A. Mehta, J. Menick, L. Metz, A. Mishchenko, P. Mishkin, V. Monaco, E. Morikawa, D. P. Mossing, T. Mu, M. Murati, O. Murk, D. M'ely, A. Nair, R. Nakano, R. Nayak, A. Neelakantan, R. Ngo, H. Noh, O. Long, C. O'Keefe, J. W. Pachocki, A. Paino, J. Palermo, A. Pantuliano, G. Parascandolo, J. Parish, E. Parparita, A. Passos, M. Pavlov, A. Peng, A. Perelman, F. de Avila Belbute Peres, M. Petrov, H. P. de Oliveira Pinto, M. Pokorny, M. Pokrass, V. H. Pong, T. Powell, A. Power, B. Power, E. Proehl, R. Puri, A. Radford, J. Rae, A. Ramesh, C. Raymond, F. Real, K. Rimbach, C. Ross, B. Rotsted, H. Roussez, N. Ryder, M. D. Saltarelli, T. Sanders, S. Santurkar, G. Sastry, H. Schmidt, D. Schnurr, J. Schulman, D. Selsam, K. Sheppard, T. Sherbakov, J. Shieh, S. Shoker, P. Shyam, S. Sidor, E. Sigler, M. Simens, J. Sitkin, K. Slama, I. Sohl, B. D. Sokolowsky, Y. Song, N. Staudacher, F. P. Such, N. Summers, I. Sutskever, J. Tang, N. A. Tezak, M. Thompson, P. Tillet, A. Tootoonchian, E. Tseng, P. Tuggle, N. Turley, J. Tworek, J. F. C. Uribe, A. Vallone, A. Vijayvergiya, C. Voss, C. Wainwright, J. J. Wang, A. Wang, B. Wang, J. Ward, J. Wei, C. Weinmann, A. Welihinda, P. Welinder, J. Weng, L. Weng, M. Wiethoff, D. Willner, C. Winter, S. Wolrich, H. Wong, L. Workman, S. Wu, J. Wu, M. Wu, K. Xiao, T. Xu, S. Yoo, K. Yu, Q. Yuan, W. Zaremba, R. Zellers, C. Zhang, M. Zhang, S. Zhao, T. Zheng, J. Zhuang, W. Zhuk, and B. Zoph. Gpt-4 technical report, 2023. URL <https://api.semanticscholar.org/CorpusID:257532815>.
- H. Ahn, J. Kwak, S. F. Lim, H. Bang, H. Kim, and T. Moon. Ss-il: Separated softmax for incremental learning. *2021 IEEE/CVF International Conference on Computer Vision (ICCV)*, pages 824–833, 2020. URL <https://api.semanticscholar.org/CorpusID:227240555>.
- R. Aljundi, P. Chakravarty, and T. Tuytelaars. Expert gate: Lifelong learning with a network of experts. In *Proceedings of the IEEE Conference on Computer Vision and Pattern Recognition*, pages 3366–3375, 2017.
- R. Aljundi, F. Babiloni, M. Elhoseiny, M. Rohrbach, and T. Tuytelaars. Memory aware synapses: Learning what (not) to forget. In *Proceedings of the European conference on computer vision (ECCV)*, pages 139–154, 2018.
- Anonymous. Imagen video: High definition video generation with diffusion models. *Submitted to Transactions on Machine Learning Research*, 2022. URL <https://openreview.net/forum?id=ETH1GDbSPw>.

- T. Brooks, B. Peebles, C. Holmes, W. DePue, Y. Guo, L. Jing, D. Schnurr, J. Taylor, T. Luhman, E. Luhman, C. Ng, R. Wang, and A. Ramesh. Video generation models as world simulators. 2024. URL <https://openai.com/research/video-generation-models-as-world-simulators>.
- P. Buzzega, M. Boschini, A. Porrello, D. Abati, and S. Calderara. Dark experience for general continual learning: a strong, simple baseline. *Advances in neural information processing systems*, 33:15920–15930, 2020.
- X. Cao, H. Lu, L. Huang, X. Liu, and M.-M. Cheng. Generative multi-modal models are good class-incremental learners. *arXiv preprint arXiv:2403.18383*, 2024.
- A. Chaudhry, P. K. Dokania, T. Ajanthan, and P. H. Torr. Riemannian walk for incremental learning: Understanding forgetting and intransigence. In *Proceedings of the European conference on computer vision (ECCV)*, pages 532–547, 2018a.
- A. Chaudhry, M. Ranzato, M. Rohrbach, and M. Elhoseiny. Efficient lifelong learning with a-gem. *arXiv preprint arXiv:1812.00420*, 2018b.
- A. Chaudhry, M. Rohrbach, M. Elhoseiny, T. Ajanthan, P. K. Dokania, P. H. Torr, and M. Ranzato. On tiny episodic memories in continual learning. *arXiv preprint arXiv:1902.10486*, 2019.
- P. Chrabaszcz, I. Loshchilov, and F. Hutter. A downsampled variant of imagenet as an alternative to the cifar datasets. *arXiv preprint arXiv:1707.08819*, 2017.
- B. Christian. *The alignment problem: How can machines learn human values?* Atlantic Books, 2021.
- Y. Cong, M. Zhao, J. Li, S. Wang, and L. Carin. Gan memory with no forgetting. *ArXiv*, abs/2006.07543, 2020a. URL <https://api.semanticscholar.org/CorpusID:219686951>.
- Y. Cong, M. Zhao, J. Li, S. Wang, and L. Carin. Gan memory with no forgetting. *Advances in Neural Information Processing Systems*, 33:16481–16494, 2020b.
- M. De Lange, R. Aljundi, M. Masana, S. Parisot, X. Jia, A. Leonardis, G. Slabaugh, and T. Tuytelaars. A continual learning survey: Defying forgetting in classification tasks. *IEEE transactions on pattern analysis and machine intelligence*, 44(7):3366–3385, 2021.
- M. Delange, R. Aljundi, M. Masana, S. Parisot, X. Jia, A. Leonardis, G. Slabaugh, and T. Tuytelaars. A continual learning survey: Defying forgetting in classification tasks. *IEEE Transactions on Pattern Analysis and Machine Intelligence*, page 1–1, 2021. ISSN 1939-3539. doi: 10.1109/tpami.2021.3057446. URL <http://dx.doi.org/10.1109/TPAMI.2021.3057446>.
- L. Deng. The mnist database of handwritten digit images for machine learning research [best of the web]. *IEEE Signal Processing Magazine*, 29(6):141–142, 2012. doi: 10.1109/MSP.2012.2211477.
- P. Dhariwal and A. Nichol. Diffusion models beat gans on image synthesis. *Advances in neural information processing systems*, 34:8780–8794, 2021a.
- P. Dhariwal and A. Nichol. Diffusion models beat gans on image synthesis, 2021b.
- K. Doan, Q. Tran, T. L. Tran, T. Nguyen, D. Phung, and T. Le. Class-prototype conditional diffusion model with gradient projection for continual learning, 2024.
- C. Donahue, J. McAuley, and M. Puckette. Adversarial audio synthesis, 2019.

- A. Douillard, M. Cord, C. Ollion, T. Robert, and E. Valle. Podnet: Pooled outputs distillation for small-tasks incremental learning. In *Computer vision–ECCV 2020: 16th European conference, Glasgow, UK, August 23–28, 2020, proceedings, part XX 16*, pages 86–102. Springer, 2020.
- C. Fernando, D. Banarse, C. Blundell, Y. Zwols, D. Ha, A. A. Rusu, A. Pritzel, and D. Wierstra. Pathnet: Evolution channels gradient descent in super neural networks. *arXiv preprint arXiv:1701.08734*, 2017.
- R. Gao and W. Liu. DDGR: Continual learning with deep diffusion-based generative replay. In A. Krause, E. Brunskill, K. Cho, B. Engelhardt, S. Sabato, and J. Scarlett, editors, *Proceedings of the 40th International Conference on Machine Learning*, volume 202 of *Proceedings of Machine Learning Research*, pages 10744–10763. PMLR, 23–29 Jul 2023. URL <https://proceedings.mlr.press/v202/gao23e.html>.
- I. J. Goodfellow, J. Pouget-Abadie, M. Mirza, B. Xu, D. Warde-Farley, S. Ozair, A. Courville, and Y. Bengio. Generative adversarial networks, 2014.
- Y. Guo, B. Liu, and D. Zhao. Dealing with cross-task class discrimination in online continual learning. In *Proceedings of the IEEE/CVF Conference on Computer Vision and Pattern Recognition*, pages 11878–11887, 2023.
- K. He, X. Zhang, S. Ren, and J. Sun. Deep residual learning for image recognition. In *2016 IEEE Conference on Computer Vision and Pattern Recognition (CVPR)*, pages 770–778, 2016. doi: 10.1109/CVPR.2016.90.
- H. Hemati, L. Pellegrini, X. Duan, Z. Zhao, F. Xia, M. Masana, B. Tscheschner, E. Veas, Y. Zheng, S. Zhao, S.-Y. Li, S.-J. Huang, V. Lomonaco, and G. M. van de Ven. Continual learning in the presence of repetition, 2024.
- M. Heusel, H. Ramsauer, T. Unterthiner, B. Nessler, and S. Hochreiter. Gans trained by a two time-scale update rule converge to a local nash equilibrium. *Advances in neural information processing systems*, 30, 2017.
- G. Hinton, O. Vinyals, and J. Dean. Distilling the knowledge in a neural network. *arXiv preprint arXiv:1503.02531*, 2015.
- J. Ho and T. Salimans. Classifier-free diffusion guidance. In *NeurIPS 2021 Workshop on Deep Generative Models and Downstream Applications*, 2021. URL <https://openreview.net/forum?id=qw8AKxfYbI>.
- J. Ho, A. Jain, and P. Abbeel. Denoising diffusion probabilistic models. *Advances in neural information processing systems*, 33:6840–6851, 2020a.
- J. Ho, A. Jain, and P. Abbeel. Denoising diffusion probabilistic models, 2020b.
- S. Hou, X. Pan, C. C. Loy, Z. Wang, and D. Lin. Learning a unified classifier incrementally via rebalancing. In *Proceedings of the IEEE/CVF conference on computer vision and pattern recognition*, pages 831–839, 2019.
- E. J. Hu, yelong shen, P. Wallis, Z. Allen-Zhu, Y. Li, S. Wang, L. Wang, and W. Chen. LoRA: Low-rank adaptation of large language models. In *International Conference on Learning Representations*, 2022. URL <https://openreview.net/forum?id=nZeVKeeFYf9>.
- C.-Z. A. Huang, A. Vaswani, J. Uszkoreit, N. Shazeer, I. Simon, C. Hawthorne, A. M. Dai, M. D. Hoffman, M. Dinculescu, and D. Eck. Music transformer, 2018.

- R. Huang, A. Geng, and Y. Li. On the importance of gradients for detecting distributional shifts in the wild. *Advances in Neural Information Processing Systems*, 34:677–689, 2021.
- P. Isola, J.-Y. Zhu, T. Zhou, and A. A. Efros. Image-to-image translation with conditional adversarial networks, 2018.
- M. Jiang, Y. Liang, X. Feng, X. Fan, Z. Pei, Y. Xue, and R. Guan. Text classification based on deep belief network and softmax regression. *Neural Computing and Applications*, 29:61 – 70, 2016. URL <https://api.semanticscholar.org/CorpusID:15946343>.
- B. Jing, G. Corso, J. Chang, R. Barzilay, and T. Jaakkola. Torsional diffusion for molecular conformer generation. In S. Koyejo, S. Mohamed, A. Agarwal, D. Belgrave, K. Cho, and A. Oh, editors, *Advances in Neural Information Processing Systems*, volume 35, pages 24240–24253. Curran Associates, Inc., 2022. URL https://proceedings.neurips.cc/paper_files/paper/2022/file/994545b2308bbbbc97e3e687ea9e464f-Paper-Conference.pdf.
- N. Kalchbrenner, E. Grefenstette, and P. Blunsom. A convolutional neural network for modelling sentences, 2014.
- T. Karras, T. Aila, S. Laine, and J. Lehtinen. Progressive growing of gans for improved quality, stability, and variation. *arXiv preprint arXiv:1710.10196*, 2017.
- T. Karras, S. Laine, and T. Aila. A style-based generator architecture for generative adversarial networks, 2019.
- T. Karras, M. Aittala, J. Hellsten, S. Laine, J. Lehtinen, and T. Aila. Training generative adversarial networks with limited data. *Advances in neural information processing systems*, 33:12104–12114, 2020a.
- T. Karras, S. Laine, M. Aittala, J. Hellsten, J. Lehtinen, and T. Aila. Analyzing and improving the image quality of StyleGAN. In *Proc. CVPR*, 2020b.
- Z. Ke and B. Liu. Continual learning of natural language processing tasks: A survey, 2023.
- Z. Ke, B. Liu, H. Wang, and L. Shu. Continual learning with knowledge transfer for sentiment classification. In *Machine Learning and Knowledge Discovery in Databases: European Conference, ECML PKDD 2020, Ghent, Belgium, September 14–18, 2020, Proceedings, Part III*, pages 683–698. Springer, 2021.
- Z. Ke, H. Lin, Y. Shao, H. Xu, L. Shu, and B. Liu. Continual training of language models for few-shot learning. In *Empirical Methods in Natural Language Processing (EMNLP)*, 2022.
- Z. Ke, Y. Shao, H. Lin, T. Konishi, G. Kim, and B. Liu. Continual pre-training of language models. In *The Eleventh International Conference on Learning Representations (ICLR-2023)*, 2023.
- R. Kemker and C. Kanan. Fearnnet: Brain-inspired model for incremental learning. *arXiv preprint arXiv:1711.10563*, 2017.
- G. Kim, B. Liu, and Z. Ke. A multi-head model for continual learning via out-of-distribution replay. In *Conference on Lifelong Learning Agents*, pages 548–563. PMLR, 2022.
- D. P. Kingma and M. Welling. Auto-encoding variational bayes. *arXiv preprint arXiv:1312.6114*, 2013.
- D. P. Kingma and M. Welling. Auto-encoding variational bayes, 2022.
- D. P. Kingma, T. Salimans, B. Poole, and J. Ho. Variational diffusion models, 2023.

- J. Kirkpatrick, R. Pascanu, N. Rabinowitz, J. Veness, G. Desjardins, A. A. Rusu, K. Milan, J. Quan, T. Ramalho, A. Grabska-Barwinska, et al. Overcoming catastrophic forgetting in neural networks. *Proceedings of the national academy of sciences*, 114(13):3521–3526, 2017.
- A. Kolesnikov, A. Dosovitskiy, D. Weissenborn, G. Heigold, J. Uszkoreit, L. Beyer, M. Minderer, M. Dehghani, N. Houlsby, S. Gelly, T. Unterthiner, and X. Zhai. An image is worth 16x16 words: Transformers for image recognition at scale. 2021.
- K. Kowsari, D. E. Brown, M. Heidarysafa, K. Jafari Meimandi, M. S. Gerber, and L. E. Barnes. Hdltext: Hierarchical deep learning for text classification. In *2017 16th IEEE International Conference on Machine Learning and Applications (ICMLA)*, pages 364–371, 2017. doi: 10.1109/ICMLA.2017.0-134.
- J. Krause, M. Stark, J. Deng, and L. Fei-Fei. 3d object representations for fine-grained categorization. In *Proceedings of the IEEE international conference on computer vision workshops*, pages 554–561, 2013.
- A. Krizhevsky, G. Hinton, et al. Learning multiple layers of features from tiny images. 2009.
- A. Krizhevsky, I. Sutskever, and G. E. Hinton. Imagenet classification with deep convolutional neural networks. In F. Pereira, C. Burges, L. Bottou, and K. Weinberger, editors, *Advances in Neural Information Processing Systems*, volume 25. Curran Associates, Inc., 2012. URL https://proceedings.neurips.cc/paper_files/paper/2012/file/c399862d3b9d6b76c8436e924a68c45b-Paper.pdf.
- N. Kumari, B. Zhang, R. Zhang, E. Shechtman, and J.-Y. Zhu. Multi-concept customization of text-to-image diffusion. In *Proceedings of the IEEE/CVF Conference on Computer Vision and Pattern Recognition*, pages 1931–1941, 2023.
- S. Lai, L. Xu, K. Liu, and J. Zhao. Recurrent convolutional neural networks for text classification. In *Proceedings of the Twenty-Ninth AAAI Conference on Artificial Intelligence, AAAI’15*, page 2267–2273. AAAI Press, 2015. ISBN 0262511290.
- Y. LeCun, C. Cortes, and C. Burges. Mnist handwritten digit database, 2010.
- J. Leike, D. Krueger, T. Everitt, M. Martic, V. Maini, and S. Legg. Scalable agent alignment via reward modeling: a research direction. *arXiv preprint arXiv:1811.07871*, 2018.
- B. Li, X. Qi, T. Lukasiewicz, and P. Torr. Controllable text-to-image generation. In H. Wallach, H. Larochelle, A. Beygelzimer, F. d’Alché-Buc, E. Fox, and R. Garnett, editors, *Advances in Neural Information Processing Systems*, volume 32. Curran Associates, Inc., 2019. URL https://proceedings.neurips.cc/paper_files/paper/2019/file/1d72310edc006dadf2190caad5802983-Paper.pdf.
- Z. Li and D. Hoiem. Learning without forgetting. *IEEE transactions on pattern analysis and machine intelligence*, 40(12):2935–2947, 2017.
- H. Lin, B. Huang, H. Ye, Q. Chen, Z. Wang, S. Li, J. Ma, X. Wan, J. Zou, and Y. Liang. Selecting large language model to fine-tune via rectified scaling law. *arXiv preprint arXiv:2402.02314*, 2024a.
- H. Lin, Y. Shao, W. Qian, N. Pan, Y. Guo, and B. Liu. Class incremental learning via likelihood ratio based task prediction. *International Conference on Learning Representations (ICLR)*, 2024b.
- B. Liu, S. Mazumder, E. Robertson, and S. Grigsby. Ai autonomy: Self-initiated open-world continual learning and adaptation. *AI Magazine*, 44(2):185–199, 2023a.

- X. Liu, C. Gong, and Q. Liu. Flow straight and fast: Learning to generate and transfer data with rectified flow. *ArXiv*, abs/2209.03003, 2022. URL <https://api.semanticscholar.org/CorpusID:252111177>.
- X. Liu, X. Zhang, J. Ma, J. Peng, and Q. Liu. InstafLOW: One step is enough for high-quality diffusion-based text-to-image generation. *ArXiv*, abs/2309.06380, 2023b. URL <https://api.semanticscholar.org/CorpusID:261697392>.
- V. Lomonaco, L. Pellegrini, A. Cossu, A. Carta, G. Graffieti, T. L. Hayes, M. De Lange, M. Masana, J. Pomponi, G. M. Van de Ven, et al. Avalanche: an end-to-end library for continual learning. In *Proceedings of the IEEE/CVF Conference on Computer Vision and Pattern Recognition*, pages 3600–3610, 2021.
- D. Lopez-Paz and M. Ranzato. Gradient episodic memory for continual learning. *Advances in neural information processing systems*, 30, 2017.
- H. Lu, G. Yang, N. Fei, Y. Huo, Z. Lu, P. Luo, and M. Ding. Vdt: General-purpose video diffusion transformers via mask modeling, 2023.
- A. Madotto, Z. Lin, Z. Zhou, S. Moon, P. Crook, B. Liu, Z. Yu, E. Cho, P. Fung, and Z. Wang. Continual learning in task-oriented dialogue systems. In M.-F. Moens, X. Huang, L. Specia, and S. W.-t. Yih, editors, *Proceedings of the 2021 Conference on Empirical Methods in Natural Language Processing*, pages 7452–7467, Online and Punta Cana, Dominican Republic, Nov. 2021. Association for Computational Linguistics. doi: 10.18653/v1/2021.emnlp-main.590. URL <https://aclanthology.org/2021.emnlp-main.590>.
- M. Masana, T. Tuytelaars, and J. Van de Weijer. Ternary feature masks: zero-forgetting for task-incremental learning. In *Proceedings of the IEEE/CVF conference on computer vision and pattern recognition*, pages 3570–3579, 2021.
- S. Masip, P. Rodriguez, T. Tuytelaars, and G. M. van de Ven. Continual learning of diffusion models with generative distillation, 2024.
- M. McCloskey and N. J. Cohen. Catastrophic interference in connectionist networks: The sequential learning problem. volume 24 of *Psychology of Learning and Motivation*, pages 109–165. Academic Press, 1989a. doi: [https://doi.org/10.1016/S0079-7421\(08\)60536-8](https://doi.org/10.1016/S0079-7421(08)60536-8). URL <https://www.sciencedirect.com/science/article/pii/S0079742108605368>.
- M. McCloskey and N. J. Cohen. Catastrophic interference in connectionist networks: The sequential learning problem. In *Psychology of learning and motivation*, volume 24, pages 109–165. Elsevier, 1989b.
- S. Minaee, N. Kalchbrenner, E. Cambria, N. Nikzad, M. Chenaghlu, and J. Gao. Deep learning based text classification: A comprehensive review, 2021.
- A. Nichol and P. Dhariwal. Improved denoising diffusion probabilistic models. *ArXiv*, abs/2102.09672, 2021. URL <https://api.semanticscholar.org/CorpusID:231979499>.
- M.-E. Nilsback and A. Zisserman. Automated flower classification over a large number of classes. In *2008 Sixth Indian conference on computer vision, graphics & image processing*, pages 722–729. IEEE, 2008.
- M. Oquab, T. Darcet, T. Moutakanni, H. Q. Vo, M. Szafraniec, V. Khalidov, P. Fernandez, D. Haziza, F. Massa, A. El-Nouby, M. Assran, N. Ballas, W. Galuba, R. Howes, P.-Y. B. Huang, S.-W. Li, I. Misra,

- M. G. Rabbat, V. Sharma, G. Synnaeve, H. Xu, H. Jégou, J. Mairal, P. Labatut, A. Joulin, and P. Bojanowski. Dinov2: Learning robust visual features without supervision. *ArXiv*, abs/2304.07193, 2023. URL <https://api.semanticscholar.org/CorpusID:258170077>.
- T. Park, M.-Y. Liu, T.-C. Wang, and J.-Y. Zhu. Semantic image synthesis with spatially-adaptive normalization, 2019.
- W. S. Peebles and S. Xie. Scalable diffusion models with transformers. *2023 IEEE/CVF International Conference on Computer Vision (ICCV)*, pages 4172–4182, 2022. URL <https://api.semanticscholar.org/CorpusID:254854389>.
- I. Pesovski, R. Santos, R. Henriques, and V. Trajkovik. Generative ai for customizable learning experiences. *Sustainability*, 16(7):3034, 2024.
- M.-C. Popescu, V. E. Balas, L. Perescu-Popescu, and N. Mastorakis. Multilayer perceptron and neural networks. *WSEAS Transactions on Circuits and Systems*, 8(7):579–588, 2009.
- A. Radford, L. Metz, and S. Chintala. Unsupervised representation learning with deep convolutional generative adversarial networks, 2016.
- A. Radford, J. Wu, R. Child, D. Luan, D. Amodei, I. Sutskever, et al. Language models are unsupervised multitask learners. *OpenAI blog*, 1(8):9, 2019.
- A. Radford, J. W. Kim, C. Hallacy, A. Ramesh, G. Goh, S. Agarwal, G. Sastry, A. Askell, P. Mishkin, J. Clark, et al. Learning transferable visual models from natural language supervision. In *International conference on machine learning*, pages 8748–8763. PMLR, 2021.
- O. Rafieian and H. Yoganarasimhan. Ai and personalization. *Artificial Intelligence in Marketing*, pages 77–102, 2023.
- A. Ramesh, M. Pavlov, G. Goh, S. Gray, C. Voss, A. Radford, M. Chen, and I. Sutskever. Zero-shot text-to-image generation, 2021.
- S.-A. Rebuffi, A. Kolesnikov, G. Sperl, and C. H. Lampert. icarl: Incremental classifier and representation learning. In *Proceedings of the IEEE conference on Computer Vision and Pattern Recognition*, pages 2001–2010, 2017.
- M. Riemer, I. Cases, R. Ajemian, M. Liu, I. Rish, Y. Tu, and G. Tesauro. Learning to learn without forgetting by maximizing transfer and minimizing interference. *arXiv preprint arXiv:1810.11910*, 2018.
- R. Rombach, A. Blattmann, D. Lorenz, P. Esser, and B. Ommer. High-resolution image synthesis with latent diffusion models, 2022.
- K. Roth, A. Lucchi, S. Nowozin, and T. Hofmann. Stabilizing training of generative adversarial networks through regularization. *Advances in neural information processing systems*, 30, 2017.
- N. Ruiz, Y. Li, V. Jampani, Y. Pritch, M. Rubinstein, and K. Aberman. Dreambooth: Fine tuning text-to-image diffusion models for subject-driven generation. In *Proceedings of the IEEE/CVF Conference on Computer Vision and Pattern Recognition*, pages 22500–22510, 2023.
- O. Russakovsky, J. Deng, H. Su, J. Krause, S. Satheesh, S. Ma, Z. Huang, A. Karpathy, A. Khosla, M. Bernstein, A. C. Berg, and L. Fei-Fei. ImageNet Large Scale Visual Recognition Challenge. *International Journal of Computer Vision (IJCV)*, 115(3):211–252, 2015. doi: 10.1007/s11263-015-0816-y.

- A. A. Rusu, N. C. Rabinowitz, G. Desjardins, H. Soyer, J. Kirkpatrick, K. Kavukcuoglu, R. Pascanu, and R. Hadsell. Progressive neural networks. *arXiv preprint arXiv:1606.04671*, 2016.
- C. Saharia, W. Chan, S. Saxena, L. Li, J. Whang, E. Denton, S. K. S. Ghasemipour, B. K. Ayan, S. S. Mahdavi, R. G. Lopes, T. Salimans, J. Ho, D. J. Fleet, and M. Norouzi. Photorealistic text-to-image diffusion models with deep language understanding, 2022.
- A. Seff, A. Beatson, D. Suo, and H. Liu. Continual learning in generative adversarial nets, 2017.
- J. Seo, J. Kang, and G. Park. Lfs-gan: Lifelong few-shot image generation. In *2023 IEEE/CVF International Conference on Computer Vision (ICCV)*, pages 11322–11332, Los Alamitos, CA, USA, oct 2023. IEEE Computer Society. doi: 10.1109/ICCV51070.2023.01043. URL <https://doi.ieeecomputersociety.org/10.1109/ICCV51070.2023.01043>.
- J. Serra, D. Suris, M. Miron, and A. Karatzoglou. Overcoming catastrophic forgetting with hard attention to the task. In *International Conference on Machine Learning*, pages 4548–4557. PMLR, 2018.
- J. Serrà, D. Surís, M. Miron, and A. Karatzoglou. Overcoming catastrophic forgetting with hard attention to the task, 2018.
- M. Shahin, F. F. Chen, and A. Hosseinzadeh. Harnessing customized ai to create voice of customer via gpt3. 5. *Advanced Engineering Informatics*, 61:102462, 2024.
- Y. Shao, Y. Guo, D. Zhao, and B. Liu. Class-incremental learning based on label generation. *arXiv preprint arXiv:2306.12619*, 2023.
- H. Shi, Z. Xu, H. Wang, W. Qin, W. Wang, Y. Wang, and H. Wang. Continual learning of large language models: A comprehensive survey. *arXiv preprint arXiv:2404.16789*, 2024.
- Z. Shi, S. Peng, Y. Xu, A. Geiger, Y. Liao, and Y. Shen. Deep generative models on 3d representations: A survey, 2023.
- H. Shin, J. K. Lee, J. Kim, and J. Kim. Continual learning with deep generative replay. *Advances in neural information processing systems*, 30, 2017.
- K. Simonyan and A. Zisserman. Very deep convolutional networks for large-scale image recognition. *CoRR*, abs/1409.1556, 2014. URL <https://api.semanticscholar.org/CorpusID:14124313>.
- U. Singer, A. Polyak, T. Hayes, X. Yin, J. An, S. Zhang, Q. Hu, H. Yang, O. Ashual, O. Gafni, D. Parikh, S. Gupta, and Y. Taigman. Make-a-video: Text-to-video generation without text-video data. In *The Eleventh International Conference on Learning Representations*, 2023. URL <https://openreview.net/forum?id=nJfy1Dvgz1q>.
- J. S. Smith, J. Tian, S. Halbe, Y.-C. Hsu, and Z. Kira. A closer look at rehearsal-free continual learning. In *Proceedings of the IEEE/CVF Conference on Computer Vision and Pattern Recognition*, pages 2409–2419, 2023.
- J. S. Smith, Y.-C. Hsu, L. Zhang, T. Hua, Z. Kira, Y. Shen, and H. Jin. Continual diffusion: Continual customization of text-to-image diffusion with c-lora, 2024.
- N. Soares and B. Fallenstein. Aligning superintelligence with human interests: A technical research agenda. *Machine Intelligence Research Institute (MIRI) technical report*, 8, 2014.
- J. Sohl-Dickstein, E. A. Weiss, N. Maheswaranathan, and S. Ganguli. Deep unsupervised learning using nonequilibrium thermodynamics, 2015.

- J. Song, C. Meng, and S. Ermon. Denoising diffusion implicit models. *arXiv preprint arXiv:2010.02502*, 2020a.
- Y. Song and S. Ermon. Improved techniques for training score-based generative models. *Advances in neural information processing systems*, 33:12438–12448, 2020.
- Y. Song, J. Sohl-Dickstein, D. P. Kingma, A. Kumar, S. Ermon, and B. Poole. Score-based generative modeling through stochastic differential equations. *arXiv preprint arXiv:2011.13456*, 2020b.
- Y. Song, J. Sohl-Dickstein, D. P. Kingma, A. Kumar, S. Ermon, and B. Poole. Score-based generative modeling through stochastic differential equations, 2021.
- A. Srivastava, L. Valkov, C. Russell, M. U. Gutmann, and C. Sutton. Veegan: Reducing mode collapse in gans using implicit variational learning. In *Neural Information Processing Systems*, 2017. URL <https://api.semanticscholar.org/CorpusID:9302801>.
- F.-K. Sun, C.-H. Ho, and H.-Y. Lee. {LAMAL}: {LA}nguage modeling is all you need for lifelong language learning. In *International Conference on Learning Representations*, 2020. URL <https://openreview.net/forum?id=Skgxcn4YDS>.
- G. Sun, W. Liang, J. Dong, J. Li, Z. Ding, and Y. Cong. Create your world: Lifelong text-to-image diffusion. *IEEE Transactions on Pattern Analysis and Machine Intelligence*, 2024.
- C. Szegedy, W. Liu, Y. Jia, P. Sermanet, S. Reed, D. Anguelov, D. Erhan, V. Vanhoucke, and A. Rabinovich. Going deeper with convolutions. In *2015 IEEE Conference on Computer Vision and Pattern Recognition (CVPR)*, pages 1–9, 2015. doi: 10.1109/CVPR.2015.7298594.
- G. Team, R. Anil, S. Borgeaud, Y. Wu, J.-B. Alayrac, J. Yu, R. Soricut, J. Schalkwyk, A. M. Dai, A. Hauth, et al. Gemini: a family of highly capable multimodal models. *arXiv preprint arXiv:2312.11805*, 2023.
- G. M. Van de Ven and A. S. Tolias. Three scenarios for continual learning. *arXiv preprint arXiv:1904.07734*, 2019.
- A. van den Oord, S. Dieleman, H. Zen, K. Simonyan, O. Vinyals, A. Graves, N. Kalchbrenner, A. Senior, and K. Kavukcuoglu. Wavenet: A generative model for raw audio, 2016.
- S. Varshney, V. K. Verma, K. SrijithP., L. Carin, and P. Rai. Cam-gan: Continual adaptation modules for generative adversarial networks. In *Neural Information Processing Systems*, 2021. URL <https://api.semanticscholar.org/CorpusID:236635024>.
- E. Verwimp, S. Ben-David, M. Bethge, A. Cossu, A. Gepperth, T. L. Hayes, E. Hüllermeier, C. Kanan, D. Kudithipudi, C. H. Lampert, et al. Continual learning: Applications and the road forward. *arXiv preprint arXiv:2311.11908*, 2023.
- J. S. Vitter. Random sampling with a reservoir. *ACM Transactions on Mathematical Software (TOMS)*, 11(1):37–57, 1985.
- C. Wah, S. Branson, P. Welinder, P. Perona, and S. Belongie. The caltech-ucsd birds-200-2011 dataset. 2011.
- F.-Y. Wang, D.-W. Zhou, L. Liu, H.-J. Ye, Y. Bian, D.-C. Zhan, and P. Zhao. Beef: Bi-compatible class-incremental learning via energy-based expansion and fusion. In *The Eleventh International Conference on Learning Representations*, 2022.

- L. Wang, X. Zhang, H. Su, and J. Zhu. A comprehensive survey of continual learning: Theory, method and application, 2023.
- Y. Wang, X. Chen, X. Ma, S. Zhou, Z. Huang, Y. Wang, C. Yang, Y. He, J. Yu, P. Yang, Y. Guo, T. Wu, C. Si, Y. Jiang, C. Chen, C. C. Loy, B. Dai, D. Lin, Y. Qiao, and Z. Liu. Lavie: High-quality video generation with cascaded latent diffusion models, 2024. URL <https://openreview.net/forum?id=p09XyFzZkc>.
- M. Wortsman, V. Ramanujan, R. Liu, A. Kembhavi, M. Rastegari, J. Yosinski, and A. Farhadi. Supermasks in superposition. In H. Larochelle, M. Ranzato, R. Hadsell, M. Balcan, and H. Lin, editors, *Advances in Neural Information Processing Systems*, volume 33, pages 15173–15184. Curran Associates, Inc., 2020a. URL https://proceedings.neurips.cc/paper_files/paper/2020/file/ad1f8bb9b51f023cdc80cf94bb615aa9-Paper.pdf.
- M. Wortsman, V. Ramanujan, R. Liu, A. Kembhavi, M. Rastegari, J. Yosinski, and A. Farhadi. Supermasks in superposition. *Advances in Neural Information Processing Systems*, 33:15173–15184, 2020b.
- C. Wu, L. Herranz, X. Liu, J. Van De Weijer, B. Raducanu, et al. Memory replay gans: Learning to generate new categories without forgetting. *Advances in neural information processing systems*, 31, 2018a.
- C. Wu, L. Herranz, X. Liu, Y. Wang, J. van de Weijer, and B. Raducanu. Memory replay gans: learning to generate images from new categories without forgetting. In *Neural Information Processing Systems*, 2018b. URL <https://api.semanticscholar.org/CorpusID:55701876>.
- T. Wu, L. Luo, Y.-F. Li, S. Pan, T.-T. Vu, and G. Haffari. Continual learning for large language models: A survey. *arXiv preprint arXiv:2402.01364*, 2024.
- H. Xiao, K. Rasul, and R. Vollgraf. Fashion-mnist: a novel image dataset for benchmarking machine learning algorithms. *CoRR*, abs/1708.07747, 2017a. URL <http://arxiv.org/abs/1708.07747>.
- H. Xiao, K. Rasul, and R. Vollgraf. Fashion-mnist: a novel image dataset for benchmarking machine learning algorithms, 2017b.
- Z. Xing, Q. Dai, H. Hu, Z. Wu, and Y.-G. Jiang. Simda: Simple diffusion adapter for efficient video generation, 2023.
- M. Xu, L. Yu, Y. Song, C. Shi, S. Ermon, and J. Tang. Geodiff: A geometric diffusion model for molecular conformation generation. In *International Conference on Learning Representations*, 2022. URL <https://openreview.net/forum?id=PzcvxEMzvQC>.
- S. Yan, J. Xie, and X. He. Der: Dynamically expandable representation for class incremental learning. In *Proceedings of the IEEE/CVF Conference on Computer Vision and Pattern Recognition*, pages 3014–3023, 2021.
- Z. Yang, D. Yang, C. Dyer, X. He, A. Smola, and E. Hovy. Hierarchical attention networks for document classification. In K. Knight, A. Nenkova, and O. Rambow, editors, *Proceedings of the 2016 Conference of the North American Chapter of the Association for Computational Linguistics: Human Language Technologies*, pages 1480–1489, San Diego, California, June 2016. Association for Computational Linguistics. doi: 10.18653/v1/N16-1174. URL <https://aclanthology.org/N16-1174>.
- W. Yin, J. Li, and C. Xiong. Contintin: Continual learning from task instructions. *arXiv preprint arXiv:2203.08512*, 2022.

- Y. Yu, A. Srivastava, and S. Canales. Conditional lstm-gan for melody generation from lyrics. *ACM Transactions on Multimedia Computing, Communications, and Applications*, 17(1):1–20, Feb. 2021. ISSN 1551-6865. doi: 10.1145/3424116. URL <http://dx.doi.org/10.1145/3424116>.
- M. Zając, K. Deja, A. Kuzina, J. M. Tomczak, T. Trzciński, F. Shkurti, and P. Miłoś. Exploring continual learning of diffusion models, 2023.
- X. Zeng, A. Vahdat, F. Williams, Z. Gojcic, O. Litany, S. Fidler, and K. Kreis. Lion: Latent point diffusion models for 3d shape generation, 2022.
- F. Zenke, B. Poole, and S. Ganguli. Continual learning through synaptic intelligence. In *International Conference on Machine Learning*, pages 3987–3995. PMLR, 2017.
- M. Zhai, L. Chen, F. Tung, J. He, M. Nawhal, and G. Mori. Lifelong gan: Continual learning for conditional image generation. *2019 IEEE/CVF International Conference on Computer Vision (ICCV)*, pages 2759–2768, 2019. URL <https://api.semanticscholar.org/CorpusID:198229709>.
- M. Zhai, L. Chen, and G. Mori. Hyper-lifelonggan: Scalable lifelong learning for image conditioned generation. *2021 IEEE/CVF Conference on Computer Vision and Pattern Recognition (CVPR)*, pages 2246–2255, 2021. URL <https://api.semanticscholar.org/CorpusID:232351216>.
- L. Zhang, A. Rao, and M. Agrawala. Adding conditional control to text-to-image diffusion models. In *Proceedings of the IEEE/CVF International Conference on Computer Vision (ICCV)*, pages 3836–3847, October 2023a.
- L. Zhang, A. Rao, and M. Agrawala. Adding conditional control to text-to-image diffusion models, 2023b.
- F. Zhu, X.-Y. Zhang, C. Wang, F. Yin, and C.-L. Liu. Prototype augmentation and self-supervision for incremental learning. In *Proceedings of the IEEE/CVF Conference on Computer Vision and Pattern Recognition*, pages 5871–5880, 2021.
- J.-Y. Zhu, T. Park, P. Isola, and A. A. Efros. Unpaired image-to-image translation using cycle-consistent adversarial networks, 2020.

A. Related Work

A.1. Generative Models

Generative Adversarial Networks. (GAN) GAN (Goodfellow et al., 2014) consists of two interacting networks: a generator and a discriminator. The generator G_{θ_g} , fed with random noise $\mathbf{z} \sim p_z$, is designed to produce images that mimic the true samples from a data distribution p_{data} closely enough to deceive the discriminator. Conversely, the discriminator D_{θ_d} attempts to discern between the authentic data points \mathbf{x} and the synthetic images $G_{\theta_g}(\mathbf{z})$ produced by the generator. The training objective for this adversarial process is formulated as follows (Goodfellow et al., 2014) :

$$\min_{\theta_g} \max_{\theta_d} [\mathbb{E}_{\mathbf{x} \sim p_{\text{data}}} \log D_{\theta_d}(\mathbf{x}) + \mathbb{E}_{\mathbf{z} \sim p_z} \log(1 - D_{\theta_d}(G_{\theta_g}(\mathbf{z})))] \quad (2)$$

Diffusion Models. Diffusion probabilistic models (Ho et al., 2020b; Sohl-Dickstein et al., 2015; Song et al., 2021) generate samples by an iterative denoising process. It defines a gradual process of adding noises, which is called the diffusion process or forward process and generate images by removing the noises step-by-step, which is referred to as the reverse process. In forward process, gaussian noises are added to \mathbf{x}_t , beginning from data \mathbf{x}_0 (Ho et al., 2020b):

$$q(\mathbf{x}_{t+1}|\mathbf{x}_t) = \mathcal{N}(\sqrt{1 - \beta_t}\mathbf{x}_t, \beta_t\mathbf{I}), \quad 0 \leq t < T \quad (3)$$

where β_t stands for the variance schedule of noise added at time t . With diffusion steps $T \rightarrow \infty$, \mathbf{x}_T virtually becomes a random noise sampled from $\mathcal{N}(0, \mathbf{I})$. In contrast, the reverse process starts from Gaussian noise $\mathbf{x}_T \sim \mathcal{N}(0, \mathbf{I})$, during which diffusion network predicts noises x_t (Ho et al., 2020b):

$$p_{\theta}(\mathbf{x}_{t-1}|\mathbf{x}_t) = \mathcal{N}(\boldsymbol{\mu}_{\theta}(\mathbf{x}_t, t), \boldsymbol{\Sigma}_{\theta}(\mathbf{x}_t, t)), \quad 0 < t \leq T \quad (4)$$

where $\epsilon_{\theta}(\mathbf{x}_t, t)$ is parameterized by a neural network and can be converted to $\boldsymbol{\mu}_{\theta}(\mathbf{x}_t, t)$ with reparameterization trick (Kingma and Welling, 2022) and $\boldsymbol{\Sigma}_{\theta}(\mathbf{x}_t, t) = \sigma_t\mathbf{I}$ under the isotropic Gaussian assumption of noises (Ho et al., 2020b). To learn the reverse process, diffusion models are trained by optimizing the variational lower bound (Kingma et al., 2023) of probability $p_{\theta}(\mathbf{x}_{0:T}) = p_{\theta}(\mathbf{x}_T)\prod_{t=1}^T p_{\theta}(\mathbf{x}_{t-1}|\mathbf{x}_t)$. One commonly used and simple loss equivalent is written as (Ho et al., 2020b):

$$L(\theta) = \mathbb{E}_{t, \mathbf{x}_0, \epsilon} \|\epsilon - \epsilon_{\theta}(\sqrt{\bar{\alpha}_t}\mathbf{x}_0 + \sqrt{1 - \bar{\alpha}_t}\epsilon, t)\|^2 \quad (5)$$

where $\epsilon \sim \mathcal{N}(0, \mathbf{I})$ and $\bar{\alpha}_t = \prod_{s=1}^t (1 - \beta_s)$. The sampling process starts from $\mathbf{x}_T \sim \mathcal{N}(0, \mathbf{I})$, iterates $t = T, \dots, 1$ and denoises according to formula (Ho et al., 2020b):

$$\mathbf{x}_{t-1} = \frac{1}{\sqrt{\alpha_t}} \left(\mathbf{x}_t - \frac{\beta_t}{\sqrt{1 - \bar{\alpha}_t}} \epsilon_{\theta}(\mathbf{x}_t, t) \right) + \sigma_t \mathbf{z} \quad (6)$$

where $\mathbf{z} \sim \mathcal{N}(0, \mathbf{I})$ if $t > 1$ else $\mathbf{z} = 0$.

A.2. Continual learning of generative models

Generative models have long been involved in continual learning, however, as an auxiliary measure in generative replay (Shin et al., 2017). Studies in settings where generative models behave as a CL agent are rather deficient. Relevant works are listed below, classified based on model architecture.

Continual Learning of GAN Since GAN (Goodfellow et al., 2014) was proposed, several works have brought out continual learning settings for GANs and incorporated different methods to overcome catastrophic forgetting. Seff et al. (2017) first integrated EWC (Kirkpatrick et al., 2017) into continual learning for GANs. Zhai et al. (2019) adopted knowledge distillation to distill knowledge from the previous model to the current model to mitigate catastrophic forgetting. Wu et al. (2018b) implemented deep generative replay (Shin et al., 2017), e.g., joint retraining and replay alignment, on a conditional GAN to avoid potential accumulate classification errors. Cong et al. (2020a) prevents forgetting by adding additional parameters to learn newly encountered tasks. Following FiLM and mAdaFM, the authors tailored these modulators for fully connected and convolutional networks to better perceive new information. Following this strategy, CAM-GAN (Varshney et al., 2021) proposed a combination of group-wise and point-wise convolutional filters to learn novel tasks while further improved CL performance by leveraging task-similarity estimation with Fisher information matrix. Hyper-LifelongGAN (Zhai et al., 2021) decomposed convolutional filters into dynamic task-specific filters generated by a filter generator and task-agnostic fixed weight components. Knowledge distillation techniques were adopted to further reduce forgetting issues. LFS-GAN (Seo et al., 2023) introduced newly proposed modulators termed LeFT, a rank-constrained weight factorization method while additional mode-seeking losses are adopted to prevent mode collapsing and enhance generation diversity.

Continual Learning of Diffusion Models Diffusion models (Ho et al., 2020b; Sohl-Dickstein et al., 2015; Song et al., 2021), a model that have been proved to be capable of high-quality image generations recent years, have also been experimented in CL. Gao and Liu (2023) trained a classifier and diffusion model bi-directional way, where the classifier is used to guide the conditional diffusion sampling. Doan et al. (2024) added trainable class prototypes to represent previous classes and utilize gradient projection in diffusion process to alleviate forgetting. In addition to classifier-guided methods, Zając et al. (2023) tested several common forgetting-prevent methods on MNIST Deng (2012) and Fashion-MNIST Xiao et al. (2017b) including experience replay, generative replay and L2 regularization, scratched the surface of continual diffusion model learning. Masip et al. (2024) introduced generative distillation process, aligning predicted noises with previous task models at each step of the reverse sampling trajectory. Smith et al. (2024) proposed C-LoRA that trained distinct self-regulated LoRA Hu et al. (2022) blocks in cross attention layers respectively for different tasks. We extend the C-LoRA method in our benchmarks to more general CLOG settings.

B. Comprehensive Results

B.1. Ablation study

In this section, we conduct a series of ablation studies on the configurations that we fixed in our benchmark experiments.

Different DDIM steps. Since a larger DDIM step, though may improve the generation quality, will result in significant inference overhead and is irrelevant to CL capability, we fix it to a small value. In our experiments, we set DDIM steps as 50 for all the DDIM-based baselines. We evaluate the CLOG baselines with a larger number of DDIM steps on CIFAR-10, and the results are in Table 4. It shows that the DDIM step as 50 can already faithfully reflect the performance of CLOG baselines without 2× or 4× computations.

Table 4 | Performance of Different DDIM Steps on CIFAR-10

DDIM Step		50	100	200
NCL	AFQ	115.60 \pm 20.51	112.41 \pm 16.62	105.34 \pm 13.65
	AIQ	108.19 \pm 15.02	96.82 \pm 8.82	95.04 \pm 6.47
	FR	107.04 \pm 27.11	104.75 \pm 21.75	95.94 \pm 18.22
ER	AFQ	132.07 \pm 8.92	132.94 \pm 2.91	131.77 \pm 2.35
	AIQ	138.22 \pm 6.12	131.59 \pm 3.84	136.80 \pm 3.82
	FR	93.81 \pm 13.71	95.53 \pm 5.78	90.00 \pm 5.49
EWC	AFQ	127.09 \pm 19.23	126.23 \pm 10.22	129.14 \pm 7.79
	AIQ	113.06 \pm 8.89	104.48 \pm 4.22	109.01 \pm 2.16
	FR	119.74 \pm 25.80	120.61 \pm 13.86	118.46 \pm 3.53
Ensemble	AFQ	36.52 \pm 0.55	35.91 \pm 0.48	37.73 \pm 0.95
	AIQ	36.57 \pm 1.57	34.97 \pm 1.70	40.70 \pm 3.52
	FR	0	0	0
C-LoRA	AFQ	60.11 \pm 6.15	61.21 \pm 5.89	63.94 \pm 5.30
	AIQ	173.43 \pm 45.28	56.67 \pm 6.21	58.54 \pm 5.33
	FR	0	0	0

Different memory sizes. In our benchmarks, we follow the existing CL works to set replay buffer sizes as 200 for small-scale CL datasets, and 5000 for large-scale ImageNet-1k. Table 5 shows the results of varying replay buffer sizes on CIFAR-10. It suggests that the performance of ER method is not sensitive to the memory size ranging from 20 to 400.

Table 5 | Performance of Different Memory Size of Experience Replay (ER)

Memory Size		20	50	100	200	400
ER	AFQ	133.65	136.11	138.15	135.47	133.83
	AIQ	109.35	133.10	110.96	113.66	137.00
	FR	96.58	100.11	102.45	97.98	95.99

Different class separation. As a dataset can be split into different numbers of tasks, here we experiment on CIFAR-10 with 2, 5, 10 tasks. The results are shown in Table 6.

Table 6 | Performance of Different Class Separation on CIFAR-10

Task number		10	5	2
NCL	AFQ	153.32	115.60	83.50
	AIQ	159.97	118.19	61.09
	FR	125.27	107.04	96.84
ER	AFQ	227.92	132.07	119.95
	AIQ	251.29	138.22	86.94
	FR	189.41	93.81	126.09
EWC	AFQ	174.98	127.09	96.50
	AIQ	167.55	113.06	67.73
	FR	149.96	119.74	123.77
Ensemble	AFQ	54.08	36.52	38.12
	AIQ	57.87	36.57	38.39
	FR	0	0	0
C-LoRA	AFQ	93.47	60.11	44.68
	AIQ	87.04	173.43	41.91
	FR	0.01	0.31	0.21

Different alignment scores. We also evaluate the concept-conditioned CLOG on another alignment score computed by DINO (Oquab et al., 2023). The results are shown in Table 7.

Table 7 | **AFQ results for concept-conditioned CLOG benchmark with different alignment scores.** The best result in each row with the same base method (DreamBooth, Custom Diffusion) is highlighted in **red**, while the second best and third best are highlighted in **blue** and **yellow**, respectively. The quality metric is the average of text and image alignment scores (*the higher value is better*). The AFQ is also averaged over 5 orders.

Metric	Model	NCL	Non-CL	KD	L2	EWC	SI	MAS	Ensemble	C-LoRA
CLIP Avg	DreamBooth	78.54 \pm 0.53	80.09\pm0.1	78.73 \pm 0.16	79.00 \pm 0.38	79.45\pm0.41	78.54 \pm 0.39	78.00 \pm 0.46	80.09\pm0.25	80.42\pm0.25
	Custom Diffusion	79.56 \pm 0.17	80.30\pm0.21	79.71 \pm 0.1	79.92 \pm 0.14	80.10\pm0.05	79.59 \pm 0.27	78.79 \pm 0.18	80.39\pm0.24	-
DINO Avg	DreamBooth	70.81 \pm 0.72	71.76\pm0.2	70.55 \pm 0.71	70.90 \pm 0.76	70.57 \pm 0.58	69.69 \pm 0.81	64.47 \pm 2.3	72.81\pm0.68	73.677\pm0.38
	Custom Diffusion	67.43 \pm 0.71	69.96\pm0.4	67.64 \pm 0.28	67.91 \pm 0.51	69.21 \pm 0.47	69.60\pm1.2	64.93 \pm 1.6	70.95\pm1.30	-

B.2. AIQ and FR Results

In this section, we present the AIQ and FR results on all benchmarks.

We can observe the average forgetting rate becomes negative in some cases on the CUB-Birds, Oxford-Flowers and Stanford-Cars datasets. This phenomenon suggests the existence of positive knowledge transfer among these datasets. Note that the FR of the ensemble and C-LoRA method is set to zero since we train a separate model for each task.

Table 8 | AIQ results for label-conditioned benchmarks.

	MNIST	Fashion-MNIST	CIFAR-10	CUB-Birds	Oxford-Flowers	Stanford-Cars	ImageNet
- GAN							
Non-CL	38.33 \pm 1.89	49.87 \pm 3.94	57.13 \pm 3.63	86.62 \pm 7.27	118.11 \pm 2.21	67.97 \pm 1.13	NA
NCL	45.50 \pm 4.41	73.49 \pm 5.27	80.23 \pm 5.46	125.13 \pm 10.88	127.18 \pm 13.54	97.77 \pm 10.44	NA
ER	37.23 \pm 6.24	61.62 \pm 10.59	173.08 \pm 3.13	180.04 \pm 6.14	151.53 \pm 12.58	159.86 \pm 4.94	NA
GR	54.19 \pm 12.55	36.13 \pm 12.30	71.66 \pm 0.67	180.82 \pm 2.02	158.24 \pm 2.65	190.07 \pm 19.21	NA
KD	39.31 \pm 0.34	69.12 \pm 3.48	80.98 \pm 4.71	135.21 \pm 8.06	131.76 \pm 13.04	102.79 \pm 9.81	NA
L2	44.01 \pm 9.44	81.90 \pm 10.70	82.65 \pm 4.54	182.36 \pm 11.50	159.24 \pm 9.57	202.29 \pm 37.37	NA
EWC	38.94 \pm 2.48	58.17 \pm 3.96	67.39 \pm 9.77	155.24 \pm 6.27	134.34 \pm 3.98	150.31 \pm 22.91	NA
SI	75.24 \pm 28.81	77.05 \pm 9.37	78.55 \pm 3.69	189.11 \pm 13.55	164.99 \pm 8.35	198.58 \pm 37.99	NA
MAS	48.93 \pm 2.05	61.70 \pm 2.27	70.24 \pm 4.03	179.28 \pm 9.21	143.04 \pm 9.29	169.43 \pm 12.43	NA
A-GEM	31.99 \pm 7.05	60.94 \pm 5.47	78.23 \pm 3.48	125.17 \pm 5.61	131.95 \pm 7.06	101.79 \pm 4.75	NA
Ensemble	10.85 \pm 3.26	27.30 \pm 1.04	44.35 \pm 2.04	177.25 \pm 3.59	148.64 \pm 6.28	232.97 \pm 6.27	NA
- Diffusion Model							
Non-CL	4.47 \pm 1.30	9.13 \pm 0.32	31.08 \pm 2.32	65.24 \pm 1.60	53.76 \pm 2.55	33.56 \pm 0.39	46.08
NCL	105.79 \pm 4.02	128.78 \pm 13.05	108.19 \pm 15.02	104.31 \pm 2.03	101.15 \pm 9.07	54.47 \pm 4.27	92.08
ER	19.76 \pm 1.02	36.91 \pm 2.13	138.22 \pm 6.12	79.46 \pm 4.26	77.44 \pm 2.09	77.75 \pm 3.06	97.16
GR	61.22 \pm 1.27	27.28 \pm 4.84	60.58 \pm 1.08	194.27 \pm 8.32	98.31 \pm 3.77	244.96 \pm 7.85	NA
KD	150.13 \pm 3.35	237.93 \pm 10.01	185.38 \pm 2.31	178.04 \pm 1.76	169.74 \pm 10.38	113.08 \pm 7.12	110.09
L2	158.51 \pm 14.52	175.01 \pm 13.47	164.06 \pm 6.92	175.35 \pm 10.14	188.30 \pm 21.85	267.73 \pm 25.74	112.21
EWC	137.11 \pm 17.60	131.18 \pm 5.44	113.06 \pm 8.89	104.53 \pm 8.63	101.60 \pm 4.54	59.11 \pm 3.80	98.19
SI	149.27 \pm 12.98	130.66 \pm 12.96	114.16 \pm 13.86	115.62 \pm 6.39	105.92 \pm 3.90	64.62 \pm 1.77	102.01
MAS	112.17 \pm 10.32	135.52 \pm 13.56	109.80 \pm 10.04	189.30 \pm 13.95	191.96 \pm 32.86	227.41 \pm 16.70	113.23
A-GEM	106.25 \pm 6.83	135.17 \pm 10.41	115.26 \pm 10.26	108.94 \pm 2.31	100.64 \pm 5.55	56.85 \pm 3.03	62.99
Ensemble	4.13 \pm 0.21	10.29 \pm 0.22	36.57 \pm 1.57	131.94 \pm 3.45	72.84 \pm 14.34	201.71 \pm 2.99	56.86
C-LoRA	140.51 \pm 4.74	229.63 \pm 5.09	173.43 \pm 45.28	186.01 \pm 23.20	288.38 \pm 7.12	269.84 \pm 29.35	73.16

Table 9 | AIQ results for the concept-conditioned CLOG benchmarks.

	Model	NCL	Non-CL	KD	L2	EWC	SI	MAS	Ensemble	C-LoRA
CLIP Avg	DreamBooth	78.40	79.07	78.57	78.75	79.43	78.73	77.87	0	0
	Custom Diffusion	79.86	79.40	79.64	79.86	79.77	-	79.39	0	-
DINO Avg	DreamBooth	73.66	73.71	72.06	73.15	73.02	72.32	69.24	0	0
	Custom Diffusion	71.89	72.87	71.55	71.94	71.88	-	70.46	0	-

Table 10 | FR results for label-conditioned CLOG benchmarks.

	MNIST	Fashion-MNIST	CIFAR-10	CUB-Birds	Oxford-Flowers	Stanford-Cars	ImageNet
- GAN							
Non-CL	5.13 \pm 4.30	10.42 \pm 7.03	5.91 \pm 1.29	-44.36 \pm 8.99	-18.58 \pm 9.94	-38.33 \pm 4.21	NA
NCL	68.91 \pm 7.78	94.67 \pm 17.44	74.34 \pm 13.26	-8.44 \pm 20.19	19.52 \pm 10.22	-32.05 \pm 7.63	NA
ER	94.27 \pm 31.22	128.76 \pm 3.26	209.16 \pm 16.74	15.72 \pm 26.08	13.42 \pm 11.76	56.72 \pm 3.45	NA
GR	120.05 \pm 45.12	110.12 \pm 24.27	112.96 \pm 10.23	101.54 \pm 15.07	56.11 \pm 13.07	85.51 \pm 25.89	NA
KD	60.64 \pm 5.64	87.50 \pm 4.45	74.82 \pm 16.83	-22.49 \pm 13.06	-3.91 \pm 15.64	-24.21 \pm 6.45	NA
L2	49.38 \pm 11.48	66.41 \pm 10.29	40.87 \pm 12.91	12.41 \pm 7.87	0.57 \pm 2.88	5.21 \pm 5.22	NA
EWC	58.96 \pm 6.14	80.06 \pm 13.34	50.91 \pm 32.37	7.16 \pm 12.56	2.30 \pm 4.31	-47.16 \pm 11.31	NA
SI	4.93 \pm 3.61	0.08 \pm 0.64	2.46 \pm 3.16	14.99 \pm 12.91	1.68 \pm 5.34	17.05 \pm 12.49	NA
MAS	52.57 \pm 15.81	72.31 \pm 7.88	32.45 \pm 8.39	9.18 \pm 10.15	4.18 \pm 7.28	-14.71 \pm 7.45	NA
A-GEM	44.45 \pm 20.32	84.84 \pm 23.35	66.91 \pm 14.49	0.48 \pm 11.85	0.45 \pm 12.30	-30.09 \pm 7.05	NA
Ensemble	0	0	0	0	0	0	0
- Diffusion Model							
Non-CL	1.82 \pm 3.74	-0.72 \pm 1.34	-2.46 \pm 0.99	-30.08 \pm 4.29	-12.73 \pm 6.43	-20.21 \pm 2.31	0.19
NCL	139.69 \pm 11.51	163.36 \pm 23.95	107.04 \pm 27.11	6.99 \pm 8.89	36.76 \pm 13.03	1.76 \pm 12.15	62.89
ER	14.70 \pm 30.99	54.18 \pm 3.92	93.81 \pm 13.71	-26.90 \pm 4.34	8.34 \pm 9.06	53.60 \pm 7.25	57.61
GR	100.28 \pm 6.87	32.37 \pm 5.54	54.74 \pm 3.98	75.37 \pm 24.00	51.59 \pm 12.10	178.51 \pm 7.15	NA
KD	70.52 \pm 11.67	58.28 \pm 19.35	17.22 \pm 24.80	14.89 \pm 8.13	35.30 \pm 32.65	-17.80 \pm 18.44	25.68
L2	202.09 \pm 35.42	193.35 \pm 15.23	132.67 \pm 24.35	25.69 \pm 6.33	26.03 \pm 34.77	1.25 \pm 20.09	21.49
EWC	192.15 \pm 29.17	161.97 \pm 25.18	119.74 \pm 25.80	24.14 \pm 15.32	45.24 \pm 5.50	0.05 \pm 3.74	69.17
SI	212.38 \pm 33.81	179.85 \pm 28.77	122.83 \pm 35.85	20.66 \pm 17.76	35.40 \pm 11.75	7.57 \pm 8.37	62.61
MAS	-0.16 \pm 0.28	0.75 \pm 0.83	0.96 \pm 0.94	0.72 \pm 0.99	-0.46 \pm 0.34	0.35 \pm 0.26	0.27
A-GEM	138.81 \pm 11.12	163.41 \pm 5.92	123.51 \pm 34.69	11.80 \pm 5.91	57.86 \pm 14.35	-0.61 \pm 1.22	62.99
Ensemble	0	0	0	0	0	0	0
C-LoRA	0	0	0	0	0	0	0

Table 11 | FR results for concept-conditioned CLOG benchmark

	Model	NCL	Non-CL	KD	L2	EWC	SI	MAS	Ensemble	C-LoRA
CLIP Avg	DreamBooth	0.6827	-0.7118	1.4377	0.4194	0.9916	1.5471	0.2172	0	0
	Custom Diffusion	0.3503	0.0846	0.256	0.0588	-0.1222	0.276	0.0049	0	0
DINO Avg	DreamBooth	2.5382	0.6054	3.3108	2.1836	3.3122	3.2506	0.3461	0	-
	Custom Diffusion	2.5568	1.5127	2.3811	1.5137	0.5065	1.1772	-0.0017	0	-

B.3. Visualization Results

We present visualization results of the generated images in this section. Figures B.1, B.2, B.3, B.4, B.5, B.6, and B.7 showcase synthesized images in the label-conditioned CLOG across the seven datasets in our benchmark. We visualize the synthesized images from the models over the last five tasks using the first class order, with images selected randomly to avoid cherry-picking. We select five representative methods to showcase the results: NCL, Non-CL, ER (replay-based), EWC (regularization-based), and Ensemble (parameter-isolation based).

As shown in the figure, a naive way of CL without additional techniques leads to severe forgetting. The regularization-based methods can preserve knowledge of previous tasks to some extent, but the results are still far from satisfying, especially as the number of learning tasks increases. Replay-based methods significantly mitigate the challenges of catastrophic forgetting. However, our empirical studies suggest that they are prone to mode collapse when training GANs, mainly due to the limited size of the replay memory. This may reveal a novel challenge in CLOG compared to traditional classification-based CL. Furthermore, the ensembling method achieves superior performance on each task on the first three datasets, including MNIST, Fashion-MNIST and CIFAR-10. Nevertheless, it synthesizes images with relatively low quality on the other three datasets (see Fig. B.4, B.5, B.6). Take Oxford-Flowers as an example, the separate model trained on each task fail to capture the correct structures of flowers, in contrast to other CL methods. This verifies our analysis that knowledge transfer among different tasks contribute to performance boost on these datasets.

Figures B.8, and B.9, showcase synthesized images in the concep-conditional CLOG with Custom Diffusion (Kumari et al., 2023) and DreamBooth (Ruiz et al., 2023) in our benchmark. We visualize the synthesized images from the models over the five tasks using the third class order, with images selected randomly to avoid cherry-picking. We select five representative methods to showcase the results: NCL, Non-CL, KD (regularization-based), EWC (regularization-based), and Ensemble (parameter-isolation-based).

A naive method of continual learning without additional techniques produces relatively high-quality images, particularly when using the DreamBooth method with more training parameters. Regularization-based methods can preserve knowledge from previous tasks to some extent, but the results are still unsatisfactory, especially as the number of learning tasks increases. For example, in Figures B.9, the EWC method shows that by the fifth task, the Custom Diffusion has almost entirely forgotten the color of the bear plushie and the blue hat decoration. Furthermore, Ensemble method achieves superior performance with both Custom Diffusion and DreamBooth.

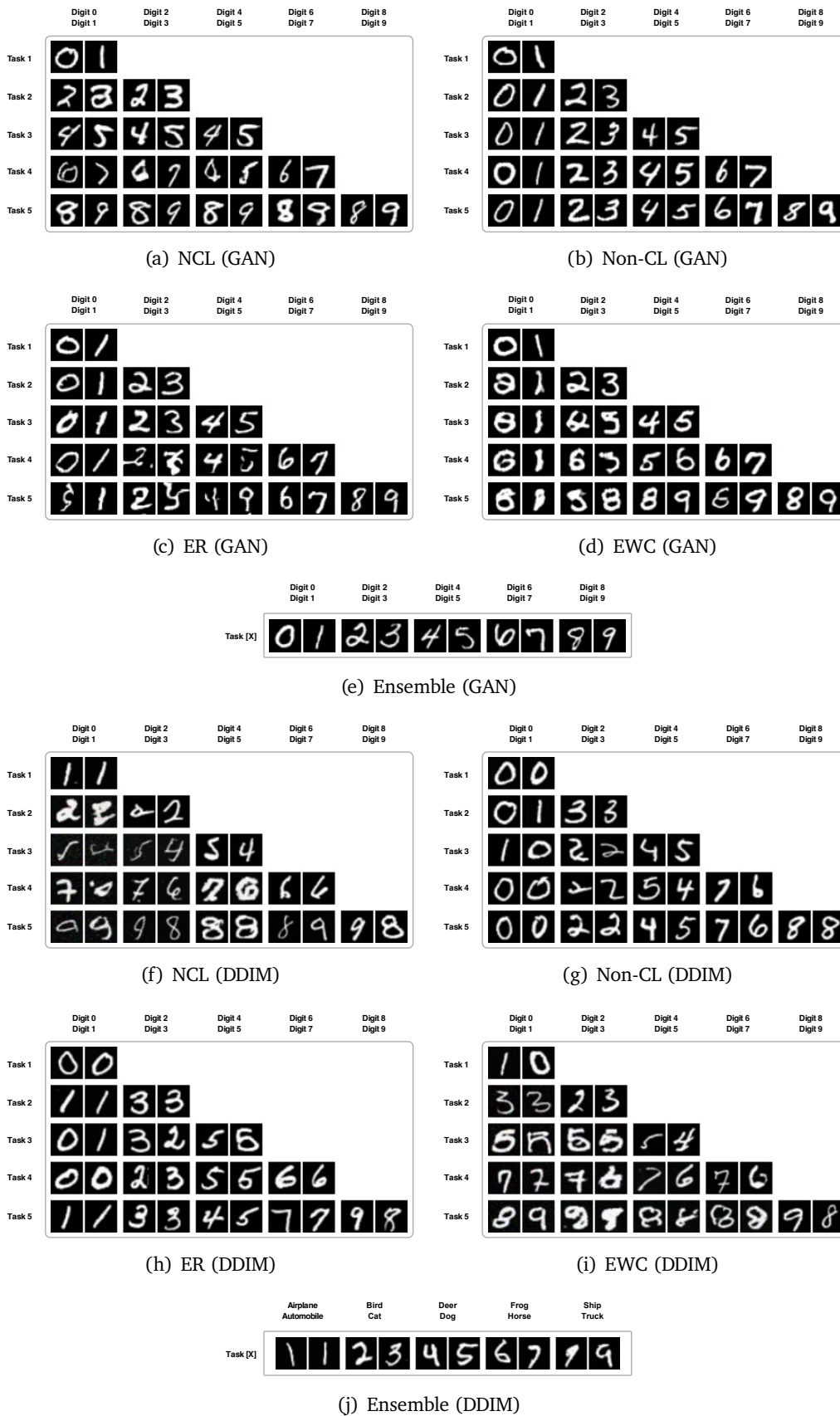


Figure B.1 | Visualization results of label-conditioned CLoG on the MNIST (Deng, 2012) dataset.

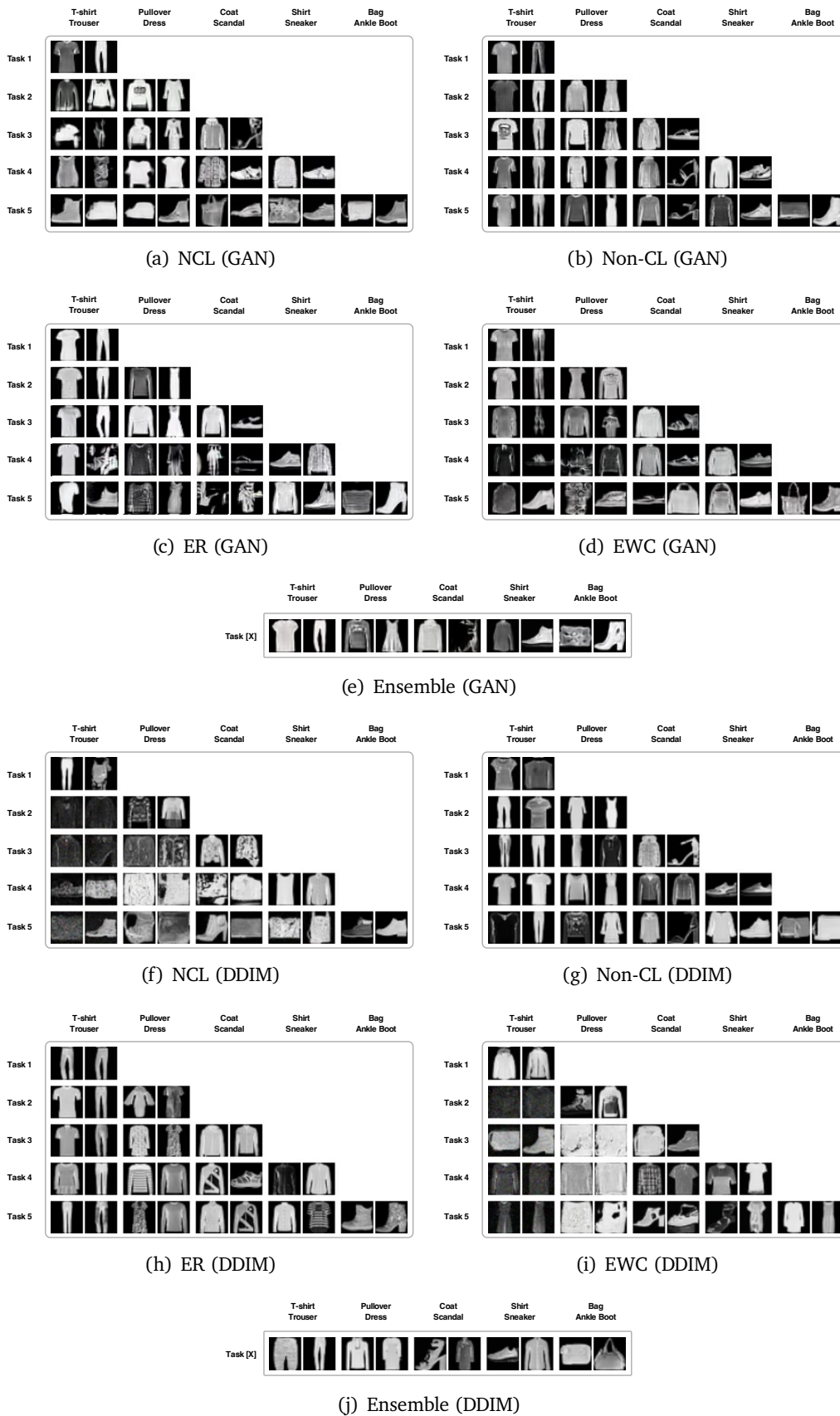


Figure B.2 | Visualization results of label-conditioned CLoG on the Fashion-MNIST (Xiao et al., 2017a) dataset.

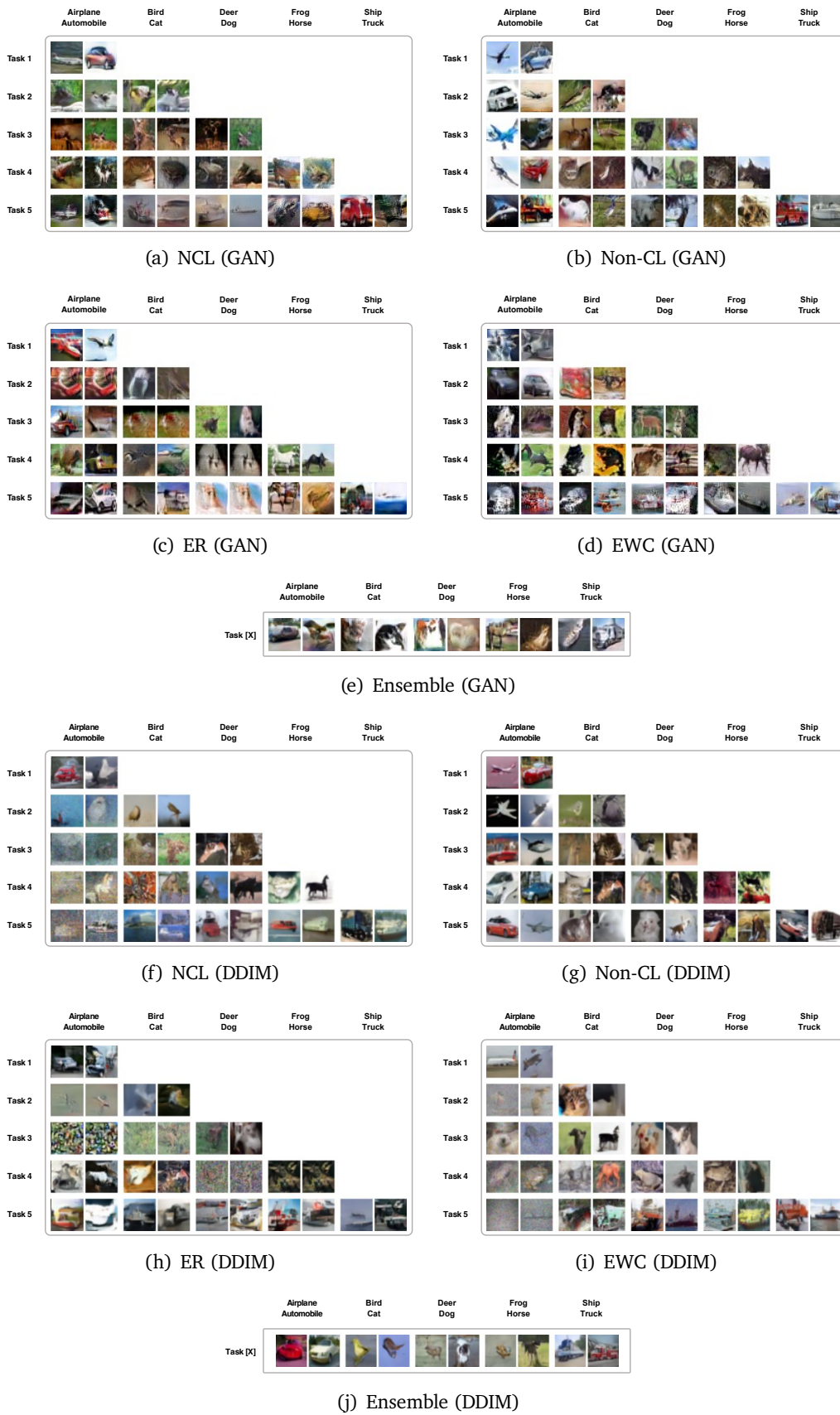


Figure B.3 | Visualization results of label-conditioned CLoG on the CIFAR-10 (Krizhevsky et al., 2009) dataset.

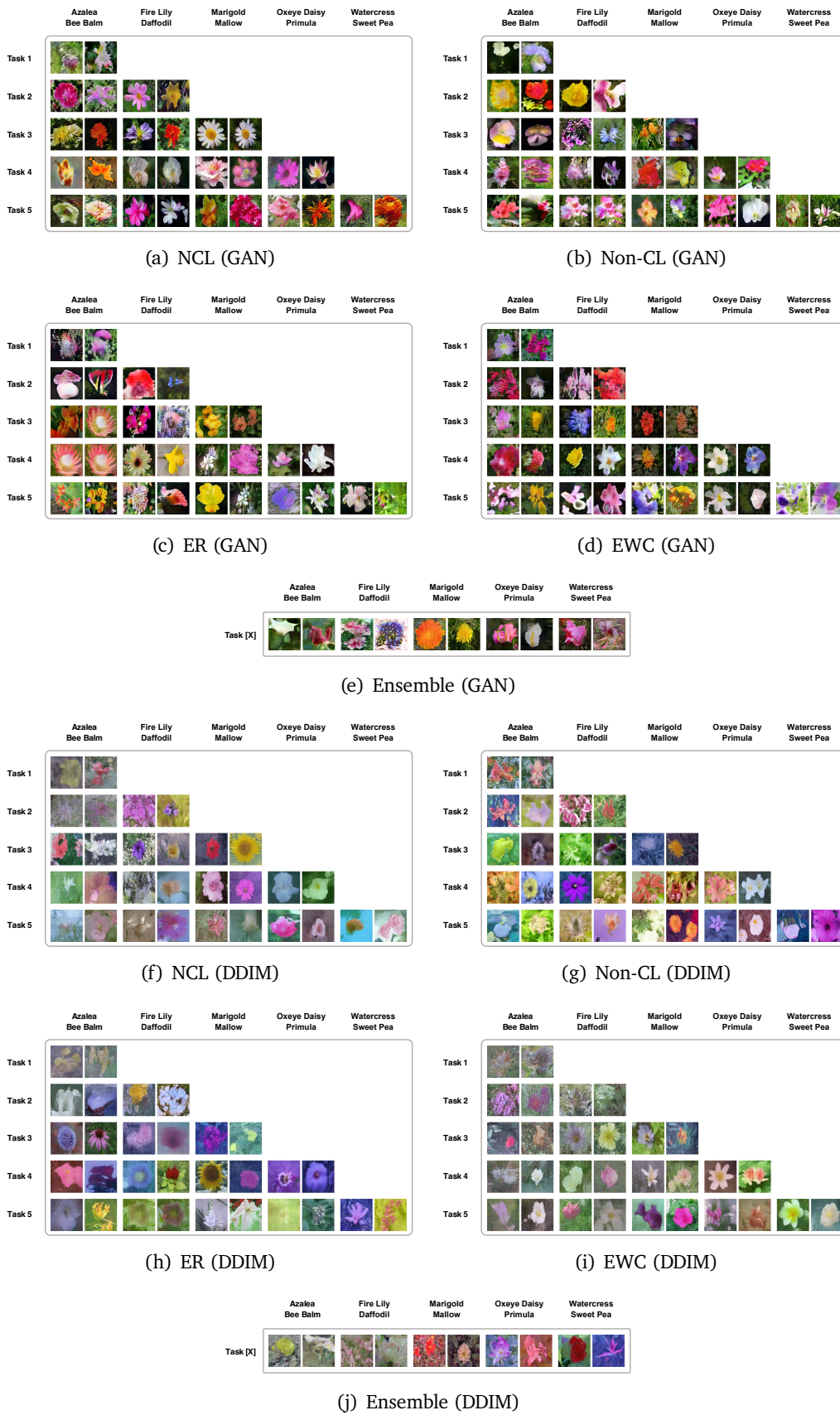


Figure B.4 | Visualization results of label-conditioned CLOG on the Oxford-Flowers (Nilsback and Zisserman, 2008) dataset.



Figure B.5 | Visualization results of label-conditioned CLOG on the CUB-Birds (Wah et al., 2011) dataset.

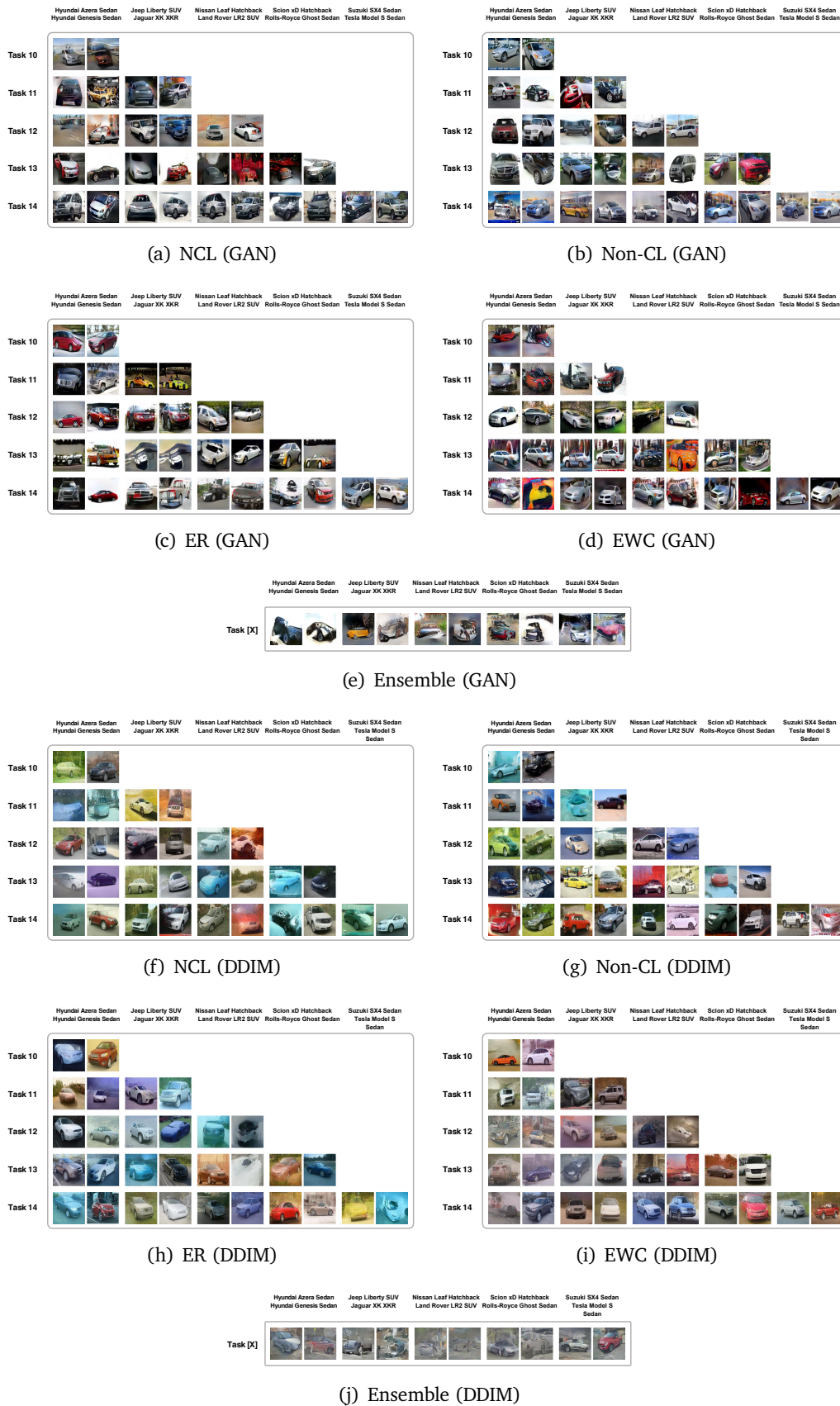


Figure B.6 | Visualization results of label-conditioned CLOG on the Stanford-Cars (Krause et al., 2013) dataset.

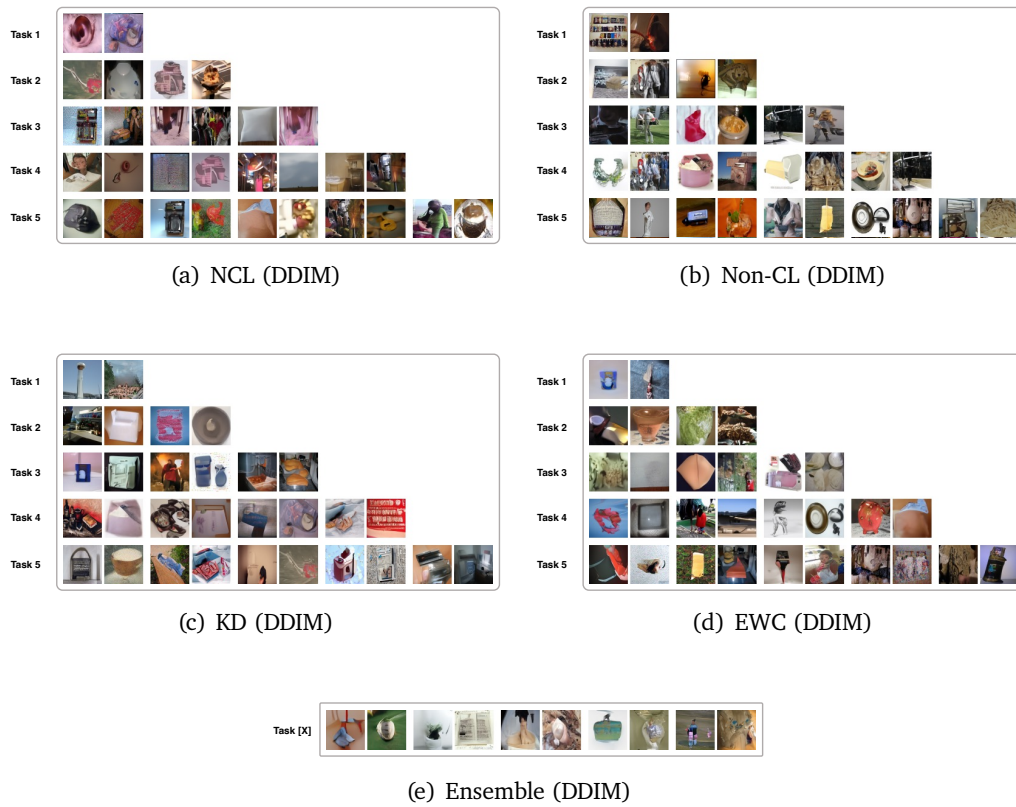


Figure B.7 | Visualization results of label-conditioned CLoG on the ImageNet-1k (Russakovsky et al., 2015) dataset.



Figure B.8 | Visualization results of concept-conditioned CLoG on the Custom Objects (Sun et al., 2024) dataset utilizing DreamBooth (Ruiz et al., 2023).



Figure B.9 | Visualization results of concept-conditioned CLoG on the Custom Objects (Sun et al., 2024) dataset utilizing Custom Diffusion (Kumari et al., 2023).

B.4. Comprehensive AIQ results for each task

To comprehensively investigate the performance of AIQ when increasing the number of learning tasks, we visualize its evolving curve in Fig. B.10 and B.11, corresponding to GANs and diffusion models, respectively. Generally, the curve exhibits an upward trend, indicating a tendency to forget the knowledge of previous tasks. However, the AIQ metric gradually decreases on the CUB-Birds, Oxford-Flowers, and Stanford-Cars datasets, demonstrating that incremental learning of similar tasks enhances performance on previous tasks.

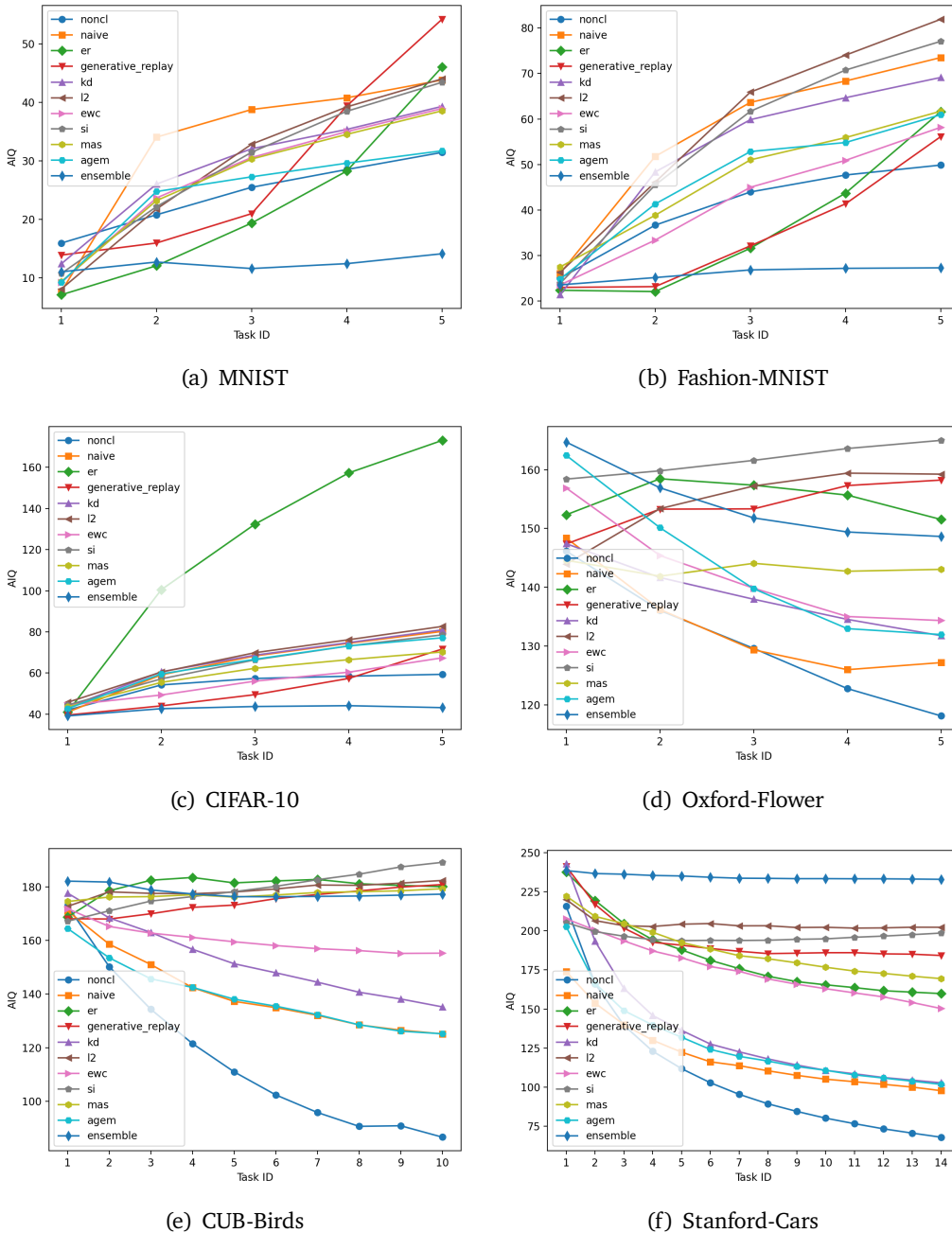
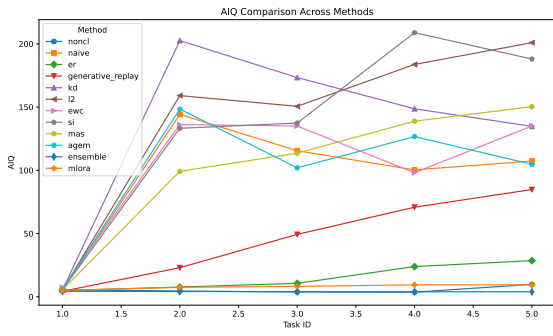
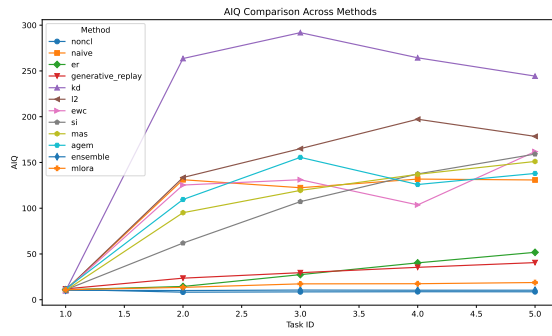


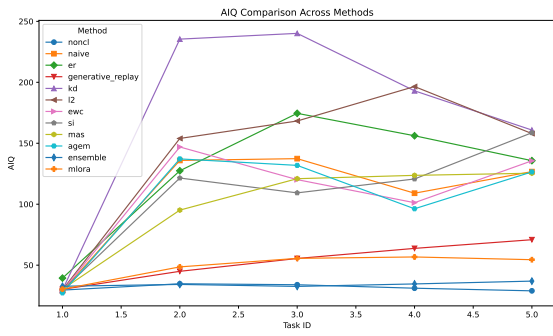
Figure B.10 | The evolving performance curve of AIQ across various tasks on label-conditioned CLoG benchmarks. Here GANs are employed as the generator backbone.



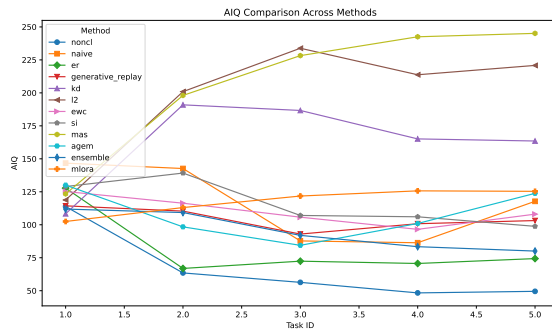
(a) MNIST (DDIM)



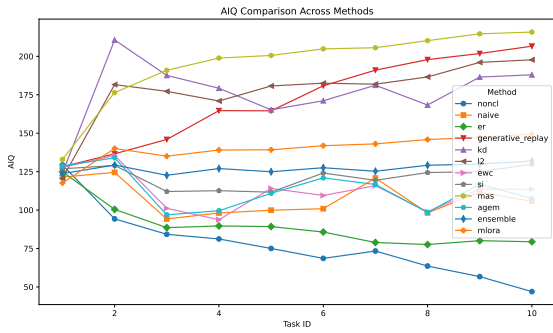
(b) Fashion-MNIST (DDIM)



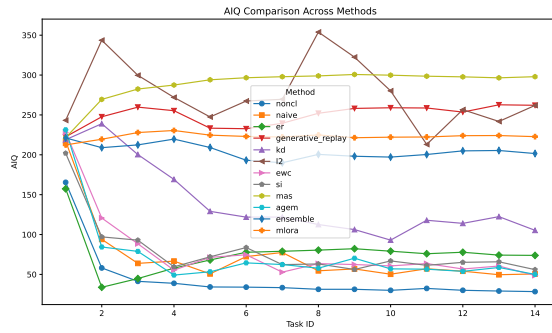
(c) CIFAR-10 (DDIM)



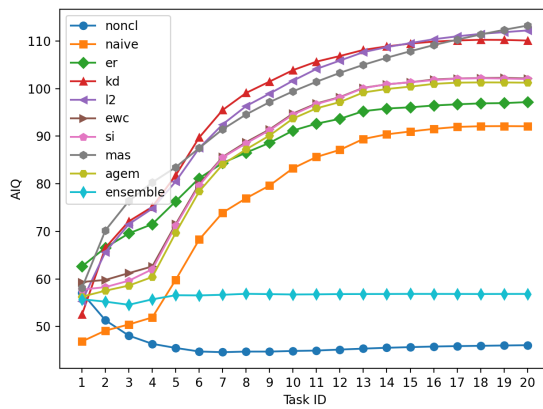
(d) Oxford-Flower (DDIM)



(e) CUB-Birds (DDIM)



(f) Stanford-Cars (DDIM)



(g) ImageNet-1k (DDIM)

Figure B.11 | The evolving performance curve of AIQ across various tasks on label-conditioned CLoG benchmarks. Here diffusion models are employed as the generator backbone.

We also visualize evolving curve in Fig. B.12 on DreamBooth and Custom Diffusion models, respectively. If we use CLIP avg to calculate AIQ, the curve exhibits an upward trend, indicating a tendency to forget the knowledge of previous tasks. On the other hand, if we use DINO avg to calculate AIQ, the metric gradually decreases for both the DreamBooth and Custom Diffusion Methods. This demonstrates that incremental learning of similar tasks enhances performance on previous tasks, which is consistent with the actual results of our generated images in Figures B.8, and B.9. We prefer the AIQ calculated by DINO avg because DINO is not trained to ignore differences between subjects of the same class. Instead, its self-supervised training objective encourages the distinction of unique features of a subject or image.

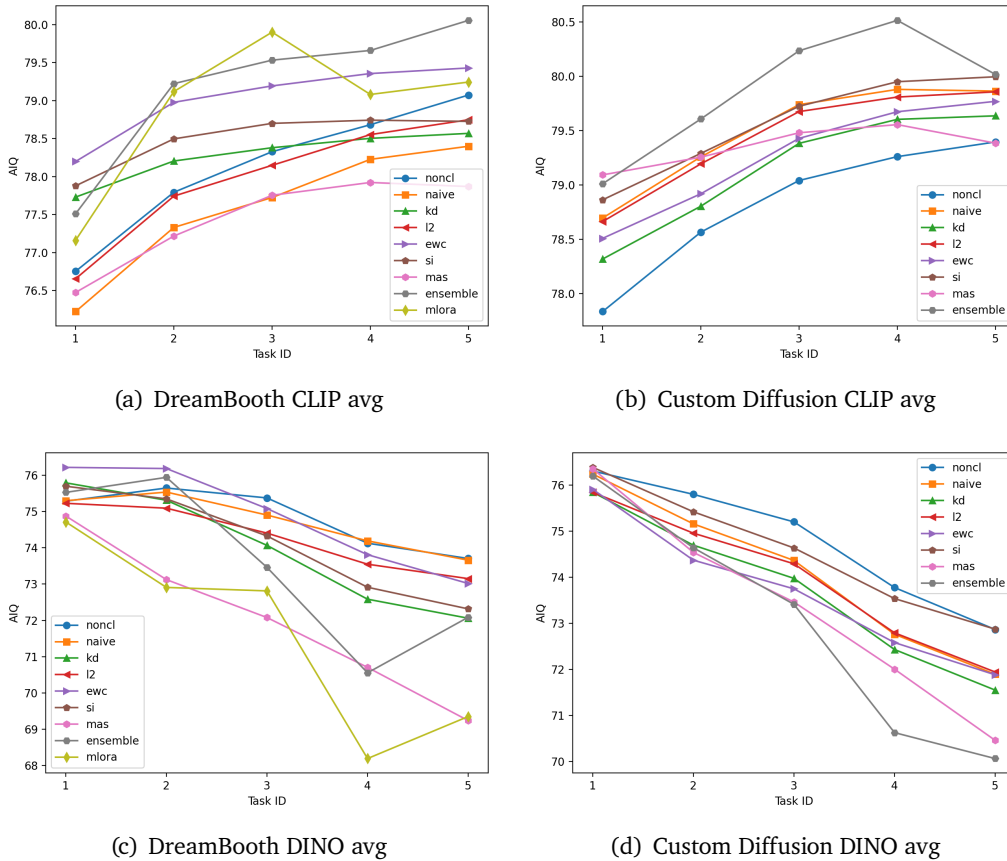


Figure B.12 | The evolving performance curve of AIQ across various tasks on concept-conditioned CLoG benchmarks. We show the results on the Custom-Objects dataset utilizing DreamBooth (Ruiz et al., 2023) and Custom Diffusion (Kumari et al., 2023).

B.5. Computational Budget Analysis

In this section, we present the memory consumption and training time for different baselines. Notice that we use a mix of different types of GPUs for different set of experiments: We use a single NVIDIA V100 GPU for GAN, a single NVIDIA RTX4090 GPU for DDIM, a single NVIDIA A100 GPU for ImageNet-1k, and a single NVIDIA A800 GPU for Costom-Objects.

Now we present a detailed analysis of memory consumption of each baseline method. Methods that require replay samples (ER and A-GEM) introduce an auxiliary replay memory to retain previous data. In addition, all regularization-methods require storing the parameters of a teacher model, doubling the total number of model parameters. Among these techniques, EWC, SI and MAS require additional computation for determining the loss weight of each parameter, resulting in a threefold increase in the model’s parameter count. Lastly, the ensemble method increases memory consumption by a factor of T (where T represents the total number of tasks), while C-LoRA introduces T additional trainable weights to facilitate conditional generation.

Table 12 | Memory Consumption of label-conditioned CLOG benchmarks: Measured in number of parameters (M)

	MNIST	Fashion-MNIST	CIFAR-10	CUB-Birds	Oxford-Flowers	Stanford-Cars	ImageNet
- GAN							
Non-CL	43.30	43.30	43.30	60.55	60.55	60.55	NA
NCL	43.30	43.30	43.30	60.55	60.55	60.55	NA
ER	43.92	43.92	43.92	70.38	70.38	70.38	NA
GR	86.60	86.60	86.60	121.10	121.10	121.10	NA
KD	86.60	86.60	86.60	121.10	121.10	121.10	NA
L2	86.60	86.60	86.60	121.10	121.10	121.10	NA
EWC	129.91	129.91	129.91	181.65	181.65	181.65	NA
SI	129.91	129.91	129.91	181.65	181.65	181.65	NA
MAS	129.91	129.91	129.91	181.65	181.65	181.65	NA
A-GEM	43.92	43.92	43.92	70.38	70.38	70.38	NA
Ensemble	216.52	216.52	216.52	605.49	302.75	847.69	NA
- Diffusion Model							
Non-CL	37.20	37.20	37.20	85.51	85.51	85.51	346.09
NCL	37.20	37.20	37.20	85.51	85.51	85.51	346.09
ER	37.40	37.40	37.40	88.71	88.71	88.71	348.55
GR	74.40	74.40	74.40	171.02	171.02	171.02	NA
KD	74.40	74.40	74.40	171.02	171.02	171.02	692.18
L2	74.40	74.40	74.40	171.02	171.02	171.02	692.18
EWC	111.60	111.60	111.60	256.53	256.53	256.53	778.71
SI	111.60	111.60	111.60	256.53	256.53	256.53	778.71
MAS	111.60	111.60	111.60	256.53	256.53	256.53	778.71
A-GEM	37.40	37.40	37.40	88.71	88.71	88.71	348.55
Ensemble	186.00	186.00	186.00	855.10	427.55	1197.74	6921.84
C-LoRA	43.00	43.00	43.00	103.11	94.31	110.15	476.45

Table 13 | Memory Consumption of concept-conditioned CLOG benchmarks: Measured in number of parameters (M)

Metric	Model	NCL	Non-CL	KD	L2	EWC	SI	MAS	Ensemble	C-LoRA
All Params	DreamBooth	1016.84	1016.84	1953.9	1953.9	2890.97	2890.97	2890.97	5084.2	1068.84
	Custom Diffusion	1035.12	1035.12	1990.47	1089.59	1144.06	1144.06	1144.06	5175.6	-
Train Params	DreamBooth	937.06	937.06	937.06	937.06	937.06	937.06	937.06	4685.3	10.4
	Custom Diffusion	54.47	54.47	54.47	54.47	54.47	54.47	54.47	272.35	-

Table 14 | Training Time of different baselines on the label-conditioned CLOG benchmark: Measured in hours over all tasks

	MNIST	Fashion-MNIST	CIFAR-10	CUB-Birds	Oxford-Flowers	Stanford-Cars	ImageNet
- GAN							
Non-CL	37.65	37.78	32.65	80.32	18.93	79.81	NA
NCL	12.81	12.62	10.82	14.78	6.26	10.64	NA
ER	16.32	15.21	12.66	16.58	7.10	11.81	NA
GR	15.76	14.96	12.78	17.30	7.18	12.20	NA
KD	15.64	15.48	13.38	16.94	7.06	12.07	NA
L2	12.92	12.69	10.74	14.96	6.38	10.51	NA
EWC	15.12	14.92	12.62	20.72	8.54	15.06	NA
SI	16.84	16.52	14.02	25.04	10.14	17.92	NA
MAS	15.16	15.12	12.74	21.17	8.72	14.93	NA
A-GEM	15.68	15.52	13.42	19.19	8.10	13.58	NA
Ensemble	12.64	12.58	10.93	14.51	6.34	10.51	NA
- Diffusion Model							
Non-CL	16.11	15.30	12.88	55.01	13.33	58.33	3953.34
NCL	2.83	3.19	3.17	3.33	3.33	6.38	103.84
ER	2.89	2.83	2.55	9.83	5.61	5.53	104.44
GR	6.9	8.83	10.22	12.64	7.89	16.80	NA
KD	3.56	2.56	3.11	7.12	6.88	8.52	135.67
L2	2.94	3.72	2.73	3.98	3.22	4.89	105.33
EWC	3.44	2.65	2.94	9.09	7.38	8.89	121.86
SI	3.89	4.64	5.05	10.72	6.64	4.59	145.86
MAS	3.96	4.14	2.89	7.37	5.94	7.22	109.44
A-GEM	3.87	3.89	2.87	13.92	12.60	10.50	104.94
Ensemble	3.34	2.67	2.22	6.12	4.94	5.83	102.31
C-LoRA	2.04	2.37	2.72	4.10	2.78	3.29	128.88

Table 15 | Training Time of different baselines on the concept-conditioned CLOG benchmark: Measured in minutes over all tasks

Model	NCL	Non-CL	KD	L2	EWC	SI	MAS	Ensemble	C-LoRA
DreamBooth	26.76	6.29	32.54	33.09	69.79	172.83	38.68	31.58	25.66
Custom Diffusion	12.40	4.02	16.65	12.49	13.33	15.45	12.25	10.15	-

C. Implementation Details

C.1. Class description

We list the class description for each label index for each dataset as follows.

- **MNIST** (10 classes)
 - digit ‘0’, digit ‘1’, digit ‘2’, digit ‘3’, digit ‘4’, digit ‘5’, digit ‘6’, digit ‘7’, digit ‘8’, digit ‘9’
- **FasionMNIST** (10 classes)
 - T-shirt/top, Trouser, Pullover, Dress, Coat, Sandal, Shirt, Sneaker, Bag, Ankle boot
- **CIFAR-10** (10 classes)
 - airplane, automobile, bird, cat, deer, dog, frog, horse, ship, truck
- **ImageNet-1k** (1,000 classes)
 - tench Tinca tinca, goldfish Carassius auratus, great white shark white shark man-eater man-eating shark Carcharodon carcharias, tiger shark Galeocerdo cuvieri, hammerhead hammerhead shark, electric ray crampfish numbfish torpedo, stingray, cock, hen, ostrich, (... 980 classes are omitted) coral fungus, agaric, gyromitra, stinkhorn carrion fungus, earthstar, hen-of-the-woods hen of the woods Polyporus frondosus Grifola frondosa, bolete, ear spike capitulum, toilet tissue toilet paper bathroom tissue
- **Oxford-Flowers** (103 classes)
 - alpine sea holly, anthurium, artichoke, azalea, ball moss, balloon flower, barbeton daisy, bearded iris, bee balm, bird of paradise, (... 980 classes are omitted), toad lily, tree mallow, tree poppy, trumpet creeper, wallflower, water lily, watercress, wild pansy, windflower, yellow iris
- **CUB-Birds** (200 classes)
 - Black footed Albatross, Laysan Albatross, Sooty Albatross, Groove billed Ani, Crested Auklet, Least Auklet, Parakeet Auklet, Rhinoceros Auklet, Brewer Blackbird, Red winged Blackbird, (... 180 classes are omitted), Red headed Woodpecker, Downy Woodpecker, Bewick Wren, Cactus Wren, Carolina Wren, House Wren, Marsh Wren, Rock Wren, Winter Wren, Common Yellowthroat
- **Stanford-Cars** (196 classes)
 - AM General Hummer SUV 2000, Acura RL Sedan 2012, Acura TL Sedan 2012, Acura TL Type-S 2008, Acura TSX Sedan 2012, Acura Integra Type R 2001, Acura ZDX Hatchback 2012, Aston Martin V8 Vantage Convertible 2012, Aston Martin V8 Vantage Coupe 2012, Aston Martin Virage Convertible 2012, (... 176 classes are omitted) Toyota Camry Sedan 2012, Toyota Corolla Sedan 2012, Toyota 4Runner SUV 2012, Volkswagen Golf Hatchback 2012, Volkswagen Golf Hatchback 1991, Volkswagen Beetle Hatchback 2012, Volvo C30 Hatchback 2012, Volvo 240 Sedan 1993, Volvo XC90 SUV 2007, smart fortwo Convertible 2012
- **Custom-Objects** (5 concepts)
 - dog, duck toy, cat, backpack, bear plushie

C.2. Random class ordering

Table 16 shows the different class orderings we used on different dataset. Due to space limitation, we only show the ordering of datasets with small class sequences. For large sequences, we refer readers to check our supplemental materials for details. The first class sequence is set as the sequence of class ordering from the original dataset, while the other sequences are generated via random shuffling.

Table 16 | The random class ordering used in our benchmarks. The full orderings can be found in our supplemental materials.

Dataset	Class order	Class sequence
MNIST, FasionMNIST, CIFAR-10	1	0, 1, 2, 3, 4, 5, 6, 7, 8, 9
	2	3, 9, 1, 8, 0, 2, 6, 4, 5, 7
	3	6, 0, 2, 8, 1, 9, 7, 3, 5, 4
	4	2, 6, 1, 5, 9, 8, 0, 4, 3, 7
	5	1, 5, 7, 2, 0, 3, 4, 6, 8, 9
Custom-Objects	1	0, 1, 2, 3, 4
	2	4, 3, 1, 0, 2
	3	4, 2, 1, 3, 0
	4	1, 4, 0, 2, 3
	5	2, 1, 0, 3, 4

C.3. Label-conditional CLOG

Implementation Details of StyleGAN2 We employ the official PyTorch implementation of StyleGAN2-ADA (Karras et al., 2020a) as our backbone. The detailed hyperparameters used in our experiments are presented in Table 17. All training runs are performed for 200 epochs using a single NVIDIA Tesla V100 GPU. We utilize six datasets with different image resolutions: 32x32 pixels (MNIST, Fashion-MNIST, CIFAR-10) and 128x128 pixels (CUB-Birds, Oxford-Flowers, Stanford-Cars). Two variants of StyleGAN2 are implemented to generate images at these resolutions, termed Ours-S and Ours-L, respectively.

We use a minibatch size of 64 for Ours-S and 16 for Ours-L. For the replay-based methods in CLOG, we construct a replay memory containing 200 samples from previous tasks, with the replay size set to one-fourth of the minibatch size (16 for Ours-S and 4 for Ours-L). Following the configuration for CIFAR-10 in the original paper (Karras et al., 2020a), we use 512 feature maps for all layers. The weight of the R_1 regularization is set to $\gamma = 0.01$ for Ours-S and $\gamma = 1$ for Ours-L. Additionally, we opt for a more expressive model architecture for the mapping network and the discriminator when synthesizing images at 128x128 pixels. Specifically, we increase the depth of the mapping network from 2 to 8 and enable residual connections in the discriminator. For simplicity, we omit several techniques that are irrelevant to CL capability used in the original paper, including adaptive discriminator augmentation (ADA), style mixing, path length regularization, and exponential moving average (EMA).

Implementation Details of DDIM We employ the Huggingface diffuser² implementation of DDIM (Song et al., 2020a) in our codebase. The detailed hyperparameters used in our experiments are presented in Table 18. All training runs are performed for 200 epochs using a single NVIDIA RTX 4090 GPU for MNIST, Fashion-MNIST, CIFAR-10, CUB-Birds, Oxford-Flowers, Stanford-Cars, and a single NVIDIA A100 GPU for the large-scale ImageNet-1k dataset. Three variants of DDIM are implemented to generate images at small resolution (32x32), medium resolution (64x64), large resolution (128x128), termed Ours-S, Ours-M, Ours-L, respectively. We use a minibatch size of 256 for Ours-S, 320 for Ours-M, 32 for Ours-L. For the replay-based methods, we maintain a replay buffer containing 200 samples from previous tasks with replay size as 64 for Ours-S and Ours-M, and 8 for Ours-L. Following Nichol and Dhariwal (2021), we use different numbers of channel and UNet blocks for Ours-S, Ours-M, and Ours-L.

²<https://huggingface.co/docs/diffusers>

Table 17 | Hyperparameters of StyleGAN2 (Karras et al., 2020a) used in our CLOG experiments.

Parameter	Ours-S	Ours-L
Resolution	32×32	128×128
Training epochs	200	200
Minibatch size	64	16
Minibatch stddev	32	32
Replay size	64	16
Memory size	200	200
Feature maps	512	512
Learning rate $\eta \times 10^3$	2.5	2.5
R_1 regularization	0.01	1
Mapping net depth	2	8
Resnet D	-	✓

Table 18 | Hyperparameters of DDIM (Song et al., 2020a) used in our CLOG experiments.

Parameter	Ours-S	Ours-M	Ours-L
Resolution	32×32	64×64	128×128
Training epochs	200	100	200
Minibatch size	256	320	32
Replay size	64	64	8
Memory size	200	5000	200
Learning rate $\eta \times 10^3$	2.0	2.0	1.0
Learning rate warm-up steps	500	500	500
Weight decay	0.0	0.0	0.0
# Unet blocks (×2)	4	4	5
Unet blocks dimension (the largest)	256	512	512
Dropout	0.1	0.1	0.1
Time embedding dimension	512	512	512

C.4. Concept-conditional CLOG

Evaluation Metrics For concept-conditioned CLOG, we follow DreamBooth (Ruiz et al., 2023) and Custom Diffusion (Kumari et al., 2023) to evaluate the alignment between generated image and the provided concept, and the text prompts, respectively. To assess subject fidelity, we use two metrics: CLIP Image Alignment and DINO Image Alignment. CLIP Image Alignment measures the average pairwise cosine similarity between the CLIP embeddings of generated and real images. Similarly, the DINO metric calculates the average pairwise cosine similarity between the ViT-S/16 DINO embeddings of generated and real images. To evaluate prompt fidelity, we compute the average cosine similarity between the CLIP embeddings of the text prompt and the images, which we refer to as CLIP Text Alignment. The averages of the image alignment and text alignment scores are combined to derive a single quality metric for straightforward comparison, labeled respectively as DINO avg and CLIP avg. We evaluate each task using 20 text prompts, generating 50 samples per prompt. This results in a total of 1,000 images generated for each task.

Implementation Details DreamBooth and Custom Diffusion both utilize generated by initial stable-diffusion-v1-4, rather than real, category images to calculate the prior loss for their training processes. 200 regularization images are preemptively created using a DDPM sampler over 50 steps with the prompt 'photo of a {category}'. We use DDPM sampling with 50 steps and a classifier-free guidance scale of 6 for both DreamBooth and Custom Diffusion. All training runs are performed using a single NVIDIA A800 GPU. More details can be found in Table 19

DreamBooth adheres to the same data augmentation strategies as Custom Diffusion, which will be introduced later, to ensure a balanced comparison. It trains by fine-tuning both a text transformer and a U-net diffusion model. This training uses a batch size of 1 and a learning rate of $2e-6$, which is maintained constant regardless of the number of GPUs or batch size. For generating target images, DreamBooth employs a text prompt formatted as 'photo of a [V] {category}', where '[V]' is replaced with a rarely used token from a specific set ('sks', 'phol', 'oxi', 'mth', 'nigh'). Each training task undergoes 800 steps. Conversely, Custom Diffusion uses a slightly different approach by setting the batch size at 2 and a scaled learning rate of $2e-5$, adjusted according to the batch size to an effective rate of $4e-5$. It trains each task for only 250 steps. During training, target images undergo random resizing: they are enlarged to between 1.2 and 1.4 times their original size every third iteration, with phrases like 'zoomed in' or 'close up' added to the text prompts. Other times, images are resized to between 0.4 and 1.0 times their original size; when the resizing ratio is below 0.6, terms like 'far away' or 'very small' are incorporated into the prompts, focusing loss propagation only within the valid image regions. The training captions, such as 'photo of a V* dog', incorporate a rare token ('ktn', 'pll', 'ucd', 'mth', 'nigh'), with both the token embedding and the cross-attention parameters being optimized during the training process.

Table 19 | Hyperparameters used in our Concept-conditional CLOG.

Parameter	DreamBooth	DreamBooth-C-LoRA	Custom Diffusion
Resolution	512×512	512×512	512×512
Training steps	800	800	250
Minibatch size	1	1	2
Inference steps	50	50	50
Learning rate	2e-6	5e-5	2e-5
Learning rate scheduler	constant	constant	constant
Learning rate warm-up steps	0	0	0
Prior loss	✓	✓	✓
Prior class images	200	200	200
Data Augmentation	✓	✓	✓

D. Impact Statement

Our work is essential as it contributes to the advancement of generative models’ continuous learning, potentially benefiting human lives and society. Our method approaches a general problem and will not have any direct negative impact or be misused in specific domains as long as the task itself is safe, ethical, and fair. The risks of these models should be evaluated based on the specific deployment context, including training data, existing guardrails, deployment environment, and authorized access.